THE ROLE OF BUTYRYLCHOLINESTERASE IN NEURAL STEM CELL DIFFERENTIATION

By

ANGELA KARIN TIETHOF

A thesis submitted to the

Graduate School-New Brunswick

and Graduate School of Biomedical Sciences

Rutgers, The State University of New Jersey

In partial fulfillment of the requirements

For the degree of

Master of Science

Graduate Program in Toxicology

Written under the direction of

Ronald P. Hart

And approved by

_____

_____

_____

_____

New Brunswick, New Jersey

January, 2017

ABSTRACT OF THE THESIS

The Role of Butyrylcholinesterase in Neural Stem Cell Differentiation

By ANGELA K. TIETHOF

Thesis Director:

Ronald P. Hart

Butyrylcholinesterase (BChE) is the evolutionary counterpart to acetylcholinesterase (AChE). Both enzymes appear early in nervous system development prior to cholinergic synapse formation. The organophosphate pesticide chlorpyrifos (CPS) primarily exerts toxicity through inhibition of AChE, which results in excess cholinergic stimulation at the synapse. We hypothesized that CPS inhibition of AChE and BChE may impair neurogenesis in neural stem cells (NSCs). To model neurodevelopment in vitro, we used human NSCs derived from induced pluripotent stem cells (iPSCs). After six days of differentiation, BChE activity and mRNA expression significantly increased, while AChE activity and expression remained unchanged. Utilizing CPS as a tool to inhibit the enzymatic activity of the enzymes resulted in 82% and 97% inhibition of AChE and BChE, respectively. CPS exposure had no obvious effect on cell morphology, viability or the expression of differentiation markers HES5, DCX or MAP2. However, shRNA-knockdown of BChE expression resulted in significantly decreased expression of bHLH transcription factors HES5 and HES3, and significantly increased expression of HES1 and the Notch pathway ligand Jagged 1 (JAG1). Results indicate BChE may have a role in the differentiation of NSCs independent of, or in addition to, its enzymatic activity.

ACKNOWLEDGEMENTS AND DEDICATION

This degree would not have been possible without the support of many people. I would like to thank my committee members Dr. Jason Richardson, Dr. Ronald Hart and Dr. Kenneth Reuhl. Their feedback and mentoring allowed me to become a better scientist, and I appreciate their support and patience during this process. I also want than Dr. Lauren Aleksunes for her caring advice and direction during this last year. Finally, I want to dedicate this degree to my loving and supportive family who have always stood by me and encouraged me with unconditional love.

TABLE OF CONTENTS

LIST OF TABLES

LIST OF FIGURES

1.0 GENERAL INTRODUCTION

1.1 Stem Cell Models

1.1.1. Stem Cell Discovery

Embryogenesis and development involves the proliferation and subsequent differentiation of stem cells. The fertilized gamete is transformed into a multicellular organism composed of specialized somatic cells. During the process of mammalian development, cells successively lose potential to differentiate into other cells types. Along this spectrum, stem cells can be described as totipotent, pluripotent or multipotent. A stem cell is defined as a cell that is self-renewing without senescence, and able to differentiate into at least one specialized cell type (Rippon and Bishop, 2004). Totipotent cells are able to differentiate into all embryonic and extra-embryonic (placental) tissues, and only early embryos in the zygote to early morula can be characterized as totipotent (Kelly, 1977). Pluripotent cells are capable of differentiating to all three embryonic germ layers: ectoderm, mesoderm and endoderm. Pluripotent cells can be obtained from embryos. The first pluripotent cells characterized were germ line carcinomas cells (Kleinsmith and Pierce, 1964). The ability to differentiate into embryonic ectoderm, mesoderm and endoderm is "proof" of pluripotency. To demonstrate human ESC pluripotency, the best test is the teratoma assay where the cells are injected into immune-compromised mice to form a differentiated cell mass containing all three germs layers (Nelakanti *et al.*, 2015). Multipotent or unipotent adult stem cells are more limited in developmental potential, but they are the basis for self renewal of tissues and are found throughout an organism.

Pluripotent embryonic stems cells (ESCs) were first isolated from mouse blastocysts (Evans and Kaufman, 1981), and several years later human ESCs were isolated and cultured (Thomson *et al.*, 1998). Mouse stem cells have been used widely in research, and they can be differentiated into multiple cell types. They were an improvement over previous pluripotent cell lines derived from teratocarcinomas called embryonal carcinoma cells (ECC) since they are karyotypically normal, and unlike ECC (Brinster, 1974), they can reliably integrate into the germ line when injected into a blastocyst (Bradley *et al.*, 1984). Mouse ESC can be injected into a blastocyst to generate a chimeric animal, which is the foundation upon which the generation of knock out or other transgenic animal models was built.

1.1.2 Neural Stem Cells

Neural tube formation is one of the earliest and most critical events in embryogenesis. Following formation of the three germ layers, the flat embryonic disk containing a layer of ectoderm know as the neural plate begins to invaginate to form the neural tube, a process called neurulation (Bear *et al.*, 2007). The closure of the neural tube follows formation of the neural groove and fusion of the neural folds, which occurs between 17 and 22 days after conception in the human embryo, with complete closure of the rostral or cephaplic end of the neural tube, termed the neuropore, on Day 24 (O'Rahilly and Muller, 1994). The neural plate becomes the walls of the neural tube, from which the cells of neural-ectoderm lineage in the CNS are derived. After neural tube formation, the different areas of CNS are patterned and formed through organized cellular proliferation, migration and differentiation.

Neural Progenitor Cells (NPCs), also known as neural stem cells (NSCs), are multipotent and can differentiate into neurons, astrocytes and oligodendrocytes (Bear *et al.*, 2007). The neural ectoderm, composed of NPCs, becomes two critical layers, named the ventricular zone and marginal zone, within the fluid filled vesicle of developing forebrain or telencephalon. Cell proliferation occurs through vertical cleavage, which expands the NPC population in the ventricular zone, or horizontal cleavage which results in cellular migration and differentiation of one daughter cell. Horizontal cleavage results in migration and differentiation because of the unequal distribution of the proteins Notch-1 and Numb, which regulate expression of transcription factors critical to cell fate determination.

Cultured ESCs can be maintained in their pluripotent state indefinitely, or they can be differentiated. The balance between the bone morphogenic protein (BMP) pathway, which inhibits neural differentiation, and FGF growth factor signaling keeps hESCs in a pluripotent state (Zhang and Li, 2005). Inhibition of the transforming growth factor-β (TGFβ) pathway (which includes BMP signaling) results in neural differentiation embryonic mammalian ectoderm and cultured mouse and human ESCs (Ozair *et al.*, 2013). Many *in vitro* NSC differentiation protocols involve inhibiting the BMP pathway. In mouse ESCs, the use of an adherent system, as opposed to an aggregate system like embryoid bodies, promotes neuroectodermal differentiation (Ying *et al.*, 2003). In the adherent system, neural rosette formation was found to be dependent on exogenous, autocrine FGF expression. The formation of a neural rosette is a key morphological change in ESC differentiation and is analogous to neural tube formation. In human ESCs, FGF promoted differentiation of embryoid bodies resulted in neural rosettes after 14 days, which further differentiated to astrocytes, neurons and oligodendrocytes upon

removal of FGF (Zhang *et al.*, 2001). Adherent, monolayer cultured hESCs can by differentiated to NPCs/NSCs using the BMP inhibitor noggin (Yao *et al.*, 2006).

1.1.3 Induced Pluripotent Stem Cells

Besides being valuable for research, human ESC can potentially be used therapeutically. Since the use of human ESC is fraught with controversy, it was desirable to find alternative ways of generating human pluripotent cells which possess the characteristics of ESCs.

During the process of differentiation, DNA undergoes epigenetic remodeling, but this process can be reversed. The genetic material contained in a somatic cell is complete, and can support embryogenesis. This was demonstrated early on, in the 1950s, by somatic cell nuclear transplant (SCNT)(Briggs and King, 1952) and later cloning experiments (Gurdon *et al.*, 1958). The transfer of a nucleus into an oocyte, or SCNT, is another way to generate stem cells, although it is technically challenging and often impractical.

The observation that mammalian cells can be reprogrammed by SCNT (Wilmut *et al.*, 2007) or by fusion with ESCs (Cowan *et al.*, 2005; Tada *et al.*, 2001) led Yamanaka to hypothesize that certain transcription factors may be utilized to reprogram a somatic cell. Takahashi and Yamanaka were able to demonstrate that over-expression of only four factors, Oct 3/4, Sox2, c-Myc and Klf4, were able to reprogram adult or embryonic mouse fibroblasts into pluripotent cells, named induced pluripotent stem cells (iPSCs)(Takahashi and Yamanaka, 2006). After perfecting mouse iPSCs conversion, they were also able to use these factors to reprogram human fibroblasts into iPSCs (Takahashi *et al.*, 2007).

The ability to produce pluripotent cells from human tissue rapidly advanced the field, and added a new aspect to stem cell research: patient specific iPSCs. One example is a study where patient specific stem cells were differentiated into functional neurons to model schizophrenia (Pedrosa *et al.*, 2011). iPSCS, like ESCs can be used to model embryogenesis and early neurodevelopment, but without the legislative limitations of existing human embryonic stem cell lines.

We have developed an adherent human iPSC-derived NSC model of early neuronal differentiation. To explore the potential of the model for DNT, we have use CPS at a concentration sufficient to inhibit both AChE and BChE. Chemical inhibition did not result in obvious perturbation during early neuronal differentiation. To test the hypothesis that BChE may have a role in neuronal differentiation separate from its enzymatic activity, we used shRNA to knockdown expression of BChE.

1.2 Acetylcholinesterase and Butyrylcholinesterase

1.2.1 History and Discovery

BChE arose from gene duplication of AChE (Chatonnet and Lockridge, 1989). The classic role of AChE in neurotransmission is well characterized (Bear *et al.*, 2007). Although BChE can compensate for AChE since it can also hydrolyze the neurotransmitter AChE at the synapse (Mesulam *et al.*, 2002), its function is less well known. Both enzymes are expressed early in development prior to establishment of a cholinergic system, and it has been hypothesized that they may play a role in early neuronal development, possibly through a non-enzymatic mechanism (Darvesh *et al.*, 2003).

Evidence for chemical neurotransmission was discovered by Otto Loewi in 1921 in a well known experiment in which fluid derived from a frog's heart after vagal-nerve stimulation, could slow or stop a denervated heart (Loewi, 1921). Loewi termed the substance "vagusstoff" which was later identified to contain an ester of choline thought to be quickly hydrolyzed *in vivo* by an enzyme. A putative cholinesterase was isolated in 1932 from horse blood (Stedman *et al.*, 1932). The preparation contained a mixture of both enzymes, named choline-esterase, as the isolate catalyzed hydrolysis of the ester ACh. It was later demonstrated that there were two enzymes present in blood. Erythrocyte cholinesterase (ChE) was distinguished by its ability to quickly catalyze ACh hydrolysis at lower physiological concentrations and by its ability to hydrolyze a synthetic substrate β-methyl acetylcholine. BChE, then known as serum ChE, was observed to be less efficient at ACh hydrolysis, although it was not inhibited at higher substrate concentrations like erythrocyte ChE and exhibited typical Michaelis-Menton kinetics (Alles and Hawes, 1940). BChE was further characterized by its ability to hydrolyze a wider range of substrates, and the term pseudo-cholinesterase was adopted (Mendel and Mundell, 1943; Mendel *et al.*, 1943; Mendel and Rudney, 1943c). ChE was shown experimentally to modulate cholinergic neurotransmission (Mendel and Hawkins, 1943), but later research only confirmed the presence of the more specific or "true" enzyme in adult vertebrate brains (Mendel and Rudney, 1943a). In 1948, more definitive studies demonstrated that erythrocyte cholinesterase hydrolyzed acetates not butyrates, whereas serum cholinesterase hydrolyzed butyrates preferentially, and the naming convention was changed to AChE and BChE, respectively (Whittaker, 2010). As AChE was thought to be the primary esterase involved in neurotransmission, the physiological role of BChE remained unclear.

1.2.2 Structure and Function of Cholinesterases

The "classical" role of AChE in cholinergic transmission is well understood (Bear *et al.*, 2007). AChE catalyzes the breakdown of ACh and terminates neurotransmission in cholinergic synapses (Fig. 1-1). ACh is synthesized in the presynaptic neuron from choline and acetyl CoA by the enzyme choline acetyl transferase (ChAT). After synthesis in the cytosol of the presynaptic terminal, neurotransmitter is loaded into vesicles by vesicular acetylcholine transporter (VAChT). After release into the synapse, AChE catalyzes the hydrolysis of ACh, and choline is recycled by active transport via the high-affinity choline transporter back into the axon terminal. Since AChE is synthesized by a variety of tissues and neuronal types, ChAT and VAChT are used as definitive markers for cholinergic neurons (Ichikawa *et al.*, 1997).

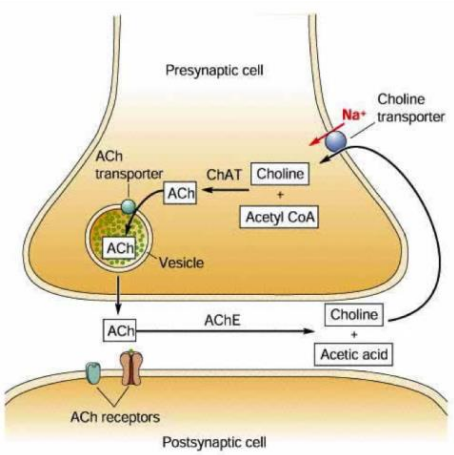

Fig. 1-1: The Cholinergic Neuron

Acetylcholine (ACh) is synthesized from acetyl CoA and choline in the presynaptic neuron. After transport into vesicles, ACh binds to receptors on the postsynaptic membrane. ACh is broken down by AChE, which terminates neuronal transmission. Image source (Bear *et al.*, 2007).

There are two subtypes of ACh receptors: nicotinic and muscarinic (Shepherd, 1994). Nicotinic receptors are ligand gated ion channel receptors found primarily at the neuromuscular junction. Muscarinic receptors are G-protein coupled receptors (GPCRs) and are found primarily in the heart. They are distinguished and named after their

respective agonists: nicotine and muscarine. Both types of receptors are also found in the central nervous system.

BChE can also hydrolyze ACh, and can compensate for AChE in knockout mice (Mesulam *et al.*, 2002), although BChE is less efficient. BChE can catalyze the hydrolysis of a wider ranges of substrates (Mendel and Rudney, 1943a), and has been shown to catalyze the hydrolysis of xenobiotics including cocaine (Gatley, 1991) and succinylcholine (Wakid *et al.*, 1985). BChE may also function as a detoxifying enzyme by scavenging anti-cholinesterase compounds like organophosphates (Chambers and Oppenheimer, 2004).

BChE and AChE have structural and functional homology, and BChE is believed to have arisen from a gene duplication of AChE early in vertebrate evolution (Chatonnet and Lockridge, 1989). They are part of the α/β fold hydrolase family of enzymes including lipases and carboxyesterases and have a common structural motif consisting of a central β-sheet surrounded by α-helices (Holmquist, 2000; Millard and Broomfield, 1992). They also have a conserved catalytic triad site consisting of a serine, histidine and glutamic acid at the bottom of a 20 Å active site gorge (Fig. 1-2). Other common features are an anionic site which bonds to the positively charged nitrogen in the choline moiety and an acyl pocket that interacts with the acyl group of the ester which together position the substrate for catalysis (Darvesh *et al.*, 2003). The enzymes also share a common mechanism: the active site serine covalently bonds to the carbonyl carbon of acetylcholine, displacing choline, forming the acyl enzyme intermediate, followed by a deacylation step where acetate is liberated. BChE has an larger acyl pocket lined by the less bulky amino acids lysine and valine, which allows for larger substrates compared to AChE (Vellom *et al.*, 1993). BChE also has a larger active site gorge volume due to less

bulky aromatic side chains, which accounts for some of the differences between the specificity of the two enzymes (Saxena *et al.*, 1999). The peripheral anionic site of AChE and BChE is located at the lip of the active site gorge, and is thought to be involved in channeling substrates to the active site, although this characteristic concentration of negative charge or "electrostatic motif" was not conserved in human BChE compared to AChE (Felder *et al.*, 1997), and the amino acids tyrosine and aspartic acid fill this role in BChE (Masson *et al.*, 1999).

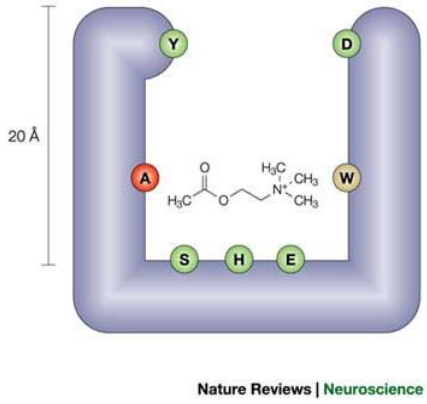

Fig. 1-2: Structure of BChE

The active site of BChE is at the bottom of a 20 Å gorge. BChE and AChE have a conserved catalytic triad that consists of the amino acids serine (S), histidine (H) and glutamic acid (G). The acyl pocket (A) and the amino acid tryptophan (W), function to position the substrate acetylcholine for catalysis. Aspartic acid (D) and tyrosine (Y) are located at the lip of the active site gorge, and compose part of the peripheral site of BChE.

Image source (Darvesh *et al.*, 2003)

AChE, a glycoprotein, consists of a catalytic core of 534 amino acids with variable C terminal length extension due to alternative splice variants (Meshorer and Soreq, 2006). The C terminal differences define the three main types of AChE: the "S" or synaptic variants, the "E" or erythrocytic variant and the "R" or read-through variant (Zimmerman and Soreq, 2006). The AChE-E form codes for a variant that is attached to the cellular membrane by a glycophospholipid link, whereas AChE-R lacks a cysteine residue so it cannot form disulfide-bonded dimers and remains soluble (Li *et al.*, 1991). The S or tailed form of AChE can exist as an amphipathic monomer, dimer or tetramer, or as homo-tetramers associated with the membrane linkage molecules of either a collagen tail (collagen Q) or proline-rich membrane linkage (PRiMA). The collagen Q linkage is

found in the neuromuscular junction whereas the PRiMA linkages are primarily found in the central nervous system (CNS). These membrane linked forms of AChE are responsible for the majority of AChE activity in the nervous system (Zimmermann, 2013).

BChE does not have multiple splice variants like AChE, and human BChE has 574 amino acid residues (Vellom *et al.*, 1993). BChE has nine sites of glycosylation compared to three in AChE (Millard and Broomfield, 1992). BChE has three globular soluble forms, G_1, G_2 and G_4, the monomer, dimer and tetramer, respectively and the tetrameric form is linked to membrane anchors PRiMA or collagen Q (See Fig. 1-3).

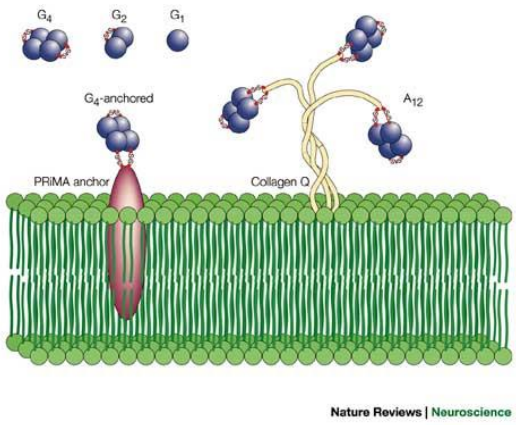

Fig. 1-3 Globular and membrane tethered forms of BChE

BChE exists as a single catalytic unit monomer (G_1), a covalently bonded dimer (G_2) or a tetramer (G_4) composed of two tetramers that associate by hydrostatic interactions. Tetramers can link with a proline-rich membrane anchor (PRiMA) or a collagen tail (collagen Q).

Image source (Darvesh *et al.*, 2003).

BChE expression differs from AChE, although some examples speak to a complementary relationship between the two enzymes. BChE is found in many tissues including the brain, whereas AChE is found in higher level in neural and muscular tissue (Massoulie, 2002). BChE is expressed in high levels in the liver and lungs, which is consistent with the hypothesis of its function as a detoxifying enzyme (Jbilo *et al.*, 1994). Soluble BChE is secreted in plasma, where it complements erythrocyte bound AChE. A collagen Q membrane linked form is found in the neuromuscular junction, further away from the immediate post synaptic membrane than AChE, in the subsynatic folds (Blondet

et al., 2010). BChE is expressed in lower levels in the adult brain than AChE, although like AChE, the enzyme exists primarily as PRiMA tetramers and is often expressed in higher concentrations in glia and astrocytes (Johnson and Moore, 2012). There is evidence for neuronal BChE in the adult brain, and BChE expressing neurons have been found in the adult human limbic system (Darvesh *et al.*, 1998).

1.2.3 Embryonic Expression and Non-Classical Function

BChE and AChE are expressed early on in embryonic development (Drews, 1975) and display characteristic spatial and temporal regulation (Layer and Sporns, 1987). In neural crests cells, BChE is expressed during mitosis followed by increased expression of AChE during migration and differentiation (Layer and Willbold, 1995). There is evidence that BChE is involved in promoting proliferation prior to differentiation (Mack and Robitzki, 2000; Robitzki *et al.*, 2000; Robitzki *et al.*, 1997), whereas AChE may be involved in neurite outgrowth and cell adhesion (Paraoanu and Layer, 2008).

Non-classical roles for AChE been reviewed extensively (Layer *et al.*, 2013; Vogel-Hopker *et al.*, 2012; Zimmerman and Soreq, 2006). To summarize, AChE or BCHE may function enzymatically in a non-classical manner to influence developmental functions by breaking down ACh during early development (prior to the establishment of cholinergic synapses), or through an alternate enzymatic "side" activities as an aryl acylamidase (Vogel-Hopker *et al.*, 2012). There is evidence that the peripheral anionic site of AChE may be involved in neurite outgrowth, since inhibitors that block the peripheral site of the enzyme change neurite outgrowth density and influence branching (Zimmerman and Soreq, 2006). Cholinesterases may interact with other proteins as a cell

adhesion molecules (CAMs), and human AChE has been shown to bind to mouse laminin-1 and human collagen IV (Johnson and Moore, 2003).

There is evidence BChE may function in early neuronal differentiation. CAMs that function in nervous system development have an extracellular domain which displays sequence homology to ChEs (Scholl and Scheiffele, 2003), and a recent x-ray crystallography structure of human BChE showed structural homology with neuroligins (Brazzolotto *et al.*, 2012). In a series of studies, 5'antisense DNA was used to drastically reduce BChE protein expression. The first two studies used an embryonic chick retinal cell system, and results indicated that BChE antisense treatment reduced proliferation and increased differentiation and apoptosis (Mack and Robitzki, 2000; Robitzki *et al.*, 1997). A supporting study was performed in a rat oligodendroglia cell line OLN-93 (Robitzki *et al.*, 2000). BChE antisense transfection reduced proliferation, upregulated protein kinase C (PKC) and pushed the cells towards an astrocytic phenotype. Finally, a more recent study used siRNA to knock down BChE in R28 cells, a retinal rat cell line with pluripotent characteristics (Bodur and Layer, 2011). Knock down of BChE increased AChE expression, and this "counter-regulation" was tightly controlled through transcription factors c-fos and P90RSK1. BChE knockdown perturbed PKC and ERK signaling suggesting that coordinated cholinesterase expression is involved in cell fate determination.

Cholinesterases are a target for pesticides and poisons that inhibit them. There are many pesticides with anti-cholinergic activity (Costa *et al.*, 2008). Since pesticides are present in low chronic doses in the environment, developmental toxicity is a concern.

1.3 The Organophosphate Pesticide Chlorpyrifos

1.3.1 History

Chlorpyrifos (CPS) is a widely used pesticide of the organophosphate class, and the toxicological effects of CPS and other organophosphate pesticides (OPs) have been extensively studied. The insecticide CPS was first registered and marketed by Dow AgroSciences 1965, and was used in the United States and throughout the world for agriculture, and also for residential and turf grass pest management and for mosquito control. Due to concerns of neurodevelopmental toxicity, use was severely curtailed in 2001. Current use in the United States is mainly on food crops including soybeans, corn and tree nuts. To minimize risk to developing human brains, use for residential and public pest management was eliminated (Eaton *et al.*, 2008). Several epidemiological studies suggest CPS exposure is correlated to adverse neurodevelopmental effects involving cognition, behavior and fetal growth (Rauh *et al.*, 2011) (Berkowitz *et al.*, 2004; Gunier *et al.*, 2016).

1.3.2 Acute Toxicity and Metabolism

CPS is classified as a "broad-spectrum chlorinated organophosphate insecticide", and the chemical name is O, O-diethyl O-(3, 5, 6,-trichloro-2 pyridyl phosphorothioate) (EPA, 2014). The mechanism of toxicity is representative of all compounds in the OP and carbamate class of pesticides (Costa *et al.*, 2008), and involves inhibiting AChE at cholinergic synapses. Activated CPS binds to the active site serine of AChE, phosphorylating the active site and inhibiting the enzyme. This inhibition is irreversible once the complex has "aged". Aging is the loss of one of the diethoxy alkyl groups of CPS. The phosphorylated complex is very stable, and AChE must be synthesized *de novo* to replace the inactivated enzyme. The primary physiological function of AChE in

the nervous system is to hydrolyze ACh. Acute toxicity results from an accumulation of ACh which leads to an over-stimulation of nicotinic and muscarinic receptors in the peripheral and central nervous system.

The set of pathological signs and symptoms that characterize an acute exposure to OPs is often referred to by the mnemonic SLUDGE which stands for Salivation, Lacrimation, Urination, Defecation, Gastric cramping and Emesis. The toxic effects can be classified as neurological, cardiovascular or respiratory, and acute exposure can result in death due to respiratory failure (Peter *et al.*, 2014). OPs generally have high acute toxicity and the oral LD50 of Chlorpyrifos in rats is between 118 to 245 mg/kg (McCollister *et al.*, 1974).

Delayed toxic effects from acute OP poisoning include an intermediate syndrome, which occurs a few days after acute exposure and organophosphate-induced delayed peripheral neuropathy (OPIDP), which usually occurs after 2 weeks (Costa *et al.*, 2008). Neither syndrome is caused directly by AChE inhibition, since they occur after recovery from acute cholinergic crises. The intermediate syndrome is characterized by weakness of respiratory muscles, neck muscles and proximal limb flexors (He *et al.*, 1998). OPIDP, distal axonopathy or degeneration of sensory and motor nerves, is a less common consequence of OP poisoning, and it is caused by inhibition and aging of a neuropathy target esterase (Lotti and Moretto, 2005).

The potential routes of exposure are inhalation, dermal and oral. CPS is well absorbed by the small intestine. Due to its hydrophobic nature, CPS may partition to the adipose tissue. CPS is known to bind plasma proteins, and metabolites can be found in

all tissues shortly after intravenous dosing. CPS and chlorpyrifos oxon (CPO; the active metabolite of CPS) cross the blood brain barrier and placenta (Eaton *et al.,* 2008).

Several enzymes are involved in the bioactivation and detoxification of CPS. CPS is converted to the active metabolite chlorpyrifos oxon (CPO) through oxidative desulfation catalyzed by cytochrome P450 enzymes (CYP), primarily CYP2B6 in human (Crane *et al.,* 2012), and a CYP2B in rats (Khokhar and Tyndale, 2012). CPO will bind to the active site serine during catalysis by AChE or BChE. Although AChE is considered the primary enzymatic target, BChE may have a role in scavenging the active metabolite, reducing the potential toxicity of CPS. Additional metabolism by Paraoxygenase 1 (PON1), an esterase, hydrolyzes and inactivates CPO. CPS can be directly detoxified by CYPs as well, particularly CYPC19 in humans. The metabolites, including the CPS-specific exposure biomarker 3, 5, 6-trichloro-2-pyrindinol (TCPy), are excreted in the urine.

1.3.3 Risk Assessment

Chlorpyrifos is a widely used pesticide, and the population is exposed to low chronic doses in the environment. In the United States, the Environmental Protection Agency (EPA) regulates pesticides. Two related laws, the Federal Insecticide, Fungicide and Rodenticide Act (FIRFA) and the Federal Food, Drug and Cosmetic Act (FFDCA), give the EPA authority to register pesticides for legal use, and establish tolerances or maximal allowable levels. In 1970, these responsibilities were transferred from the USDA and FDA to the EPA. Today, pesticide regulation is primarily the domain of the EPA, although the FDA and USDA are still involved in enforcement and/or testing (Costa, 2008).

The Food Quality and Protection Act (FQPA) of 1996 introduced further changes to pesticide regulations (Costa, 2008). Pesticides are no longer legally defined as a food additive, excluding them from the Delaney clause of the FFDCA that states that "no additive shall be deemed safe if it is found to induce cancer when ingested by man or animal". Pesticides may not be classified as food additives, but there are tolerances for the levels found in residues of foods. The EPA must also consider "aggregate" exposure or the summation of exposure from food, environment, drinking water, etc. Finally, the EPA must assess the risks to children and infants, and a 10-fold safety factor must be applied if adequate data is not available. Also, pesticides, like CPS, registered before 1984 must be re-registered, and new studies must be performed and evaluated to demonstrate safety.

The CPS Human Health Risk Assessment (EPA, 2014) used a physiologically based pharmacokinetic-pharmacodynamics (PBPK-PD) modeling and a response endpoint of 10% erythrocyte AChE inhibition to determine the point of departure (Pod) and the intra and interspecies uncertainty factors for both CPS and its active metabolite, CPO. The uncertainty factors determined do not apply to vulnerable populations including infants, children and women of childbearing age. Due to the weight of evidence (WOE), the 10x FQPA safety factor was retained for these populations since the pesticide can potentially cause developmental neurotoxicity (DNT) at doses below that which causes 10% inhibition of erythrocyte AChE. The evidence considered included *in vivo* toxicology studies that evaluated behavior and cognition, epidemiological studies and mechanistic studies including in vitro studies. There was insufficient evidence to determine a mode of action and subsequent adverse outcome pathway (MOA/AOP) for the DNT of CPS/CPO. Several plausible mechanisms distinct from AChE inhibition have been

proposed including binding to muscarinic receptors (Liu *et al.*, 1999), tubulin (Grigoryan and Lockridge, 2009) or AChE at the peripheral anionic site (Campanha *et al.*, 2014) and disrupting key cellular processes during early brain development including differentiation, migration, proliferation, neurite outgrowth and intracellular signaling.

1.3.4 Developmental Neurotoxicity

Many *in vivo* studies have been performed to evaluate the DNT of CPS including endpoints evaluating motor activity, cognition, emotion/anxiety and social interaction. Exposures above 1 mg/kg/day during development are sufficient to cause DNT in animal models (EPA, 2014). When 1 and 5 mg/kg/day CPS is administered to rats on gestational day (GD) 17-20 during the peak of neurogenesis, persistent alterations in behavior were found in offspring with differences between males and females (Levin *et al.*, 2002). A 5 mg/kg dose in mice between GD 7.5-11.5 resulted in morphological changes including thinning of CA1 and CA3 layers of the somatosensory cortex, enlargement of the dentate gyrus of the hippocampus and a decrease in the ratio of neurons and glia in the somatosensory cortex (Chen *et al.*, 2009). Similar morphological changes were found in juvenile rats after prenatal CPS exposure (Roy *et al.*, 2005). These finding were supported by recent epidemiological data which compared high and low prenatal exposure groups and found brain changes by MRI imaging including frontal and parietal cortical thinning (Rauh *et al.*, 2012).

AChE may have a role in morphogenesis of neurons, not as result of its catalytic activity, but rather as a result of AChE's interactions with other unknown cellular factors. In one study (Yang *et al.*, 2008), neurons from the dorsal root ganglia in the rat were isolated and exposed to CPS or CPO *in vitro*. Axonal growth was measured

microscopically. Axonal growth was reduced in concentrations as low as 0.001 μM for CPS, and between 0.001 and 0.01 nM CPO. The low concentrations required for this "morphogenic" exposure are below measurable enzymatic inhibition of AChE activity. Neurons from AChE null mice were also obtained. CPS/CPO did not inhibit growth of axons derived from null mice. Transfection with wild type AChE restored the sensitivity of the neurons to CPS/CPO. Site directed mutagenesis techniques demonstrated a functional active site was required for AChE-inhibition of morphogenic effects. The authors speculate that although the morphogenic effect is separate from the catalytic effect of AChE, the overall protein conformation is dependent on the presence of the active site serine. These effects were observed at CPS concentrations well below AChE inhibition, supporting a non-enzymatic role for AChE in development.

Another study (Slotkin *et al.*, 2008) investigated the effects of CPS on the expression of neurotrophic factors using a both an *in vitro* (PC12 cells) and an *in vivo* rat model. The alteration in the expression of these factors, including fibroblast growth factor (FGF) and other neurotrophins, is proposed as an underlying cause of the neurodevelopmental effects observed below the level of detectable AChE inhibition. Using microarray analysis, expression of FGF family genes was similar both *in vitro* and *in vivo*, but effects on brain-derived neurotrophic factor (BDNF) and nerve growth factor (NGF) were only seen in the *in vitro* model. Neurotrophic factors are proteins involved in the key processes of brain development including proliferation, differentiation, apoptosis, synaptogenesis and myelination (Reichardt, 2006). Disturbances in the expression of these proteins may be implicated in CPS DNT. In other words, the mechanism of acute toxicity may be caused by an increase of acetylcholine in the synapse, but the DNT may

be caused, in part, by the dysregulation in the expression of genes involved in early development.

1.0 MATERIALS AND METHODS

2.1 Generation of Induced Pluripotent Stem Cells and Neural Stem Cells

Human foreskin fibroblasts were converted to iPSCs using retroviruses of to over-express transcription factors Oct 3/4, Sox2, c-Myc and Klf4 (Takahashi *et al.*, 2007) and were grown using feeder free methodology (Ludwig *et al.*, 2006).

To obtain neural stem cells, a protocol based on a previously published methodology was used (Goff *et al.*, 2009). In addition, Noggin was utilized to inhibit the BMP pathways and promote differentiation of iPSCs to NSCs (Gerrard *et al.*, 2005). The iPSCS were plated at a density of 1:5 on BD Matrigel™ hESC-qualified matrix diluted in DMEM/F12 (354277, BD Biosciences). Cells were fed every other day with media consisting of 50% MTeSR (Stem Cell Technologies) and 50% Neural Basal Media (NBM). NBM consists of Neurobasal® Medium (21103049, Gibco), 2% B27® Supplement, 1% Insulin-Transferrin-Selenium (41400045; Gibco), 1% N2 Supplement (17502048, Gibco), 2 mM L-Glutamine (25030-081, Gibco), 0.5% Penicillin Streptomycin (15070-063, Gibco) and 500 ng/mL Noggin (120-10C; Peprotech). Five days after passage, media was changed to 100% NBM with 500 ng/mL Noggin and the media was refreshed every other day for 10 days or until culture was 90% confluent. Cells were then passage with the EZ passage tool, and single cells were removed by use of an inverted cell strainer. Cells were then plated 1:4 onto dishes coated with 20 µg/mL

laminin (L2020, Sigma) in NBM without Noggin. At approximately 60-70% confluence, about 18 days after initial passage, NSCs were switched to proliferation media (see below) and grown until about 90% confluent prior to continued passaging or differentiation.

2.2 Neural Stem Cell Culture, Differentiation and Chlorpyrifos Exposure

NSCs were cultured in proliferation media containing 20 ng/mL Recombinant Human Fibroblast Growth Factor-basic (FGF, 100-18B, PeproTech) with the following composition: 50% DMEM/F12 with glutamax (10565018, Gibco), 50% Neurobasal® Medium (21103049, Gibco) and ½ strength of both N2 Supplement 100X (17502048, Gibco) and B27® Supplement (50 X), minus vitamin A (12587010, Gibco). Cells were plated on ¼ strength BD Matrigel™ hESC-qualified matrix diluted in DMEM/F12 (354277, BD Biosciences), and passaged with Accutase™ Cell Detachment Solution (07920, Stemcell Technologies, Inc.) at 80-90% confluence at a 1:3 density (approximately 40, 000 cells/cm^2) every 3-4 days. Media was refreshed every other day. All cultures were incubated at 37 °C at 5% CO_2.

For differentiation and exposure experiments (Fig. 3-1a) cells were plated in T75 culture flasks at a density of approximately 13,500 cells/cm^2 and allowed to grow to confluence for 4-5 days. On Day 0, cultures were switched to differentiation media containing 10 ng/ml Recombinant Human Brain Derived Neurotrophic Factor (BDNF, 450-02, PeproTech) in Neurobasal plus N2 Supplement (100X) to induce differentiation. Cells were harvested using Accutase™ Cell Detachment Solution at Day 0 (prior to differentiation), Day 2, Day 4 and 6. The cell pellet was resuspended in phosphate buffered saline (PBS) and split as follows: 1/3 was used for RNA harvesting for qPCR

and 2/3 was used for enzyme assays. The suspension was centrifuged to pellet the cells. Pelleted cells were rinsed well using PBS and residual PBS was aspirated well prior freezing at ≤ -70 °C. The pellets for RNA were resuspended in 600 µL Buffer RLT (Qiagen) containing 1% β-mercaptoethanol to lyse cells, and the lysate was frozen on dry ice and stored at ≤ -70 °C.

Cells were exposed continuously to CPS 10 µM (PS-647, Chem Service Inc.) starting on Day 0 of differentiation. A stock solution of 30 mM was prepared in 100% ethanol. The stock was diluted in ethanol to 10 mM, and then added at a ratio of 1 µL per 1 mL of differentiation media. Culture media was changed every other day during scheduled collection time points. Media for control cultures contained 1 µL/mL of 100% ethanol.

2.3 Lentivirus Production and shRNA Knockdown

HEK 293T cells were cultured in Dulbecco's modified Eagle's medium with high glucose (11995, Gibco) supplemented with 10% Fetal Bovine Serum (F2442, Sigma) and 1% of the following: Penicillin Streptomycin (15070-063, Gibco), L-Glutamine (25030-081, Gibco) and Non-Essential Amino Acids (11140-050, Gibco). Cells were transfected at approximately 60% confluence the day after plating on 0.1% gelatin coated 15 cm dishes at a density of 30,000 cells/cm^2. For BChE knockdown the Mission® shRNA TRC2 lentiviral vector plasmid was purchased from Sigma (TRC number TRCN0000427955, Clone ID NM_000055.2-439s21c1) along with non-target shRNA control plasmid SHC216. Addgene 3rd generation packaging plasmids were transfected at a ratio of 4:2:1:1 of target vector, MDLg/RRE, VSVg-MD2g and RSV-REV, respectively. The DNA precipitate was formed by adding drop wise 1 mL 0.25M $CaCl_2$ solution contain 60 µg plasmid DNA into 1 mL 2x HEPES buffered saline (50 mM

HEPES pH 7.05, 140 mM NaCl, 1.4 mM Na_2HPO_4) while vortexing. The precipitate was allowed to incubate for 15-20 min. at room temperature and was then mixed with an equal volume of medium. This solution was added drop wise to the cell culture plates. The culture media was changed daily, harvested for virus on day 2 and 3 (at approximately 48 and 72 post transfection) and stored at 4 °C. The media was then centrifuged at 200g to remove cellular debris. The resulting supernatant was collected in Ultra-Clear™ centrifuge tubes (34405, Beckman Coulter). Lentivirus was concentrated by centrifuging at 25,000 rpm for 2 hours using a Beckman Coulter Optima L-90K Ultracentrifuge with a SW28 rotor. The supernatant was removed completely and virus was resuspended in 180 µL DMEM/F12 overnight and stored at ≤ -70 °C prior to use.

To quantify virus the Sigma-Aldrich Lentiviral Titer via p24 ELISA assay protocol was used and the viral supernatants were assayed using the Retrotek HIV-1 p24 Antigen ELISA (0801111, Zeptometrix Corp.). Viral concentration was quantified as transducing units (TU) per mL.

For knockdown experiments, cultures were seeded at a density of approximately 13,500 cells/cm^2 in 6 well plate culture dishes. The following day, cultures were transfected with a volume of lentivirus containing 6 TU per cell in proliferation media containing 8 µg/mL protamine sulfate (P3369, Sigma Aldrich). Media was changed the next day to remove virus and protamine sulfate, and lysates for RNA were collected on Day 0 and Day 6 of differentiation. Two wells of a 6 wells plate were pooled for each viral treatment (Control and BChE knockdown). Wells were rinsed twice with PBS prior to lysing with 600 µL Buffer RLT containing 1% β-mercaptoethanol. The lysate was frozen on dry ice and stored at ≥ -70 °C prior to RNA isolation.

2.4 Quantitative Real-time Polymerase Chain Reaction

RNA was isolated using the RNeasy® Mini Kit (Qiagen) following RNeasy® Mini Handbook instructions. Lysates were thawed on ice and homogenized using a rotor-stator homogenizer. On column DNase treatment was performed as per kit instructions using the RNase-Free DNase set (79254, Qiagen). RNA was quantified using a NanoDrop, and 0.8 µg RNA was reverse transcribed using SuperScript™ First-Strand Synthesis System for RT-PCR (11901-018, Invitrogen) following directions for first-strand synthesis using random primers.

Quantitative-PCR (qPCR) was performed using a ViiA™ 7 Real Time PCR system (Applied Biosytems) and Power SYBR® Green PCR Master Mix (4367659, Applied Biosystems). A 25 µL reaction volume was assayed in duplicate 10 µL volumes in an optically clear 384 well reaction plate. The 25 µL reaction contained 12.5 µL of 2x SYBR®Green PCR Master mix, cDNA template and a 0.2 µM concentration of each primer (0.4 µM total primer concentration). Thermal cycling conditions were as follows: 2 min. at 50 °C and 10 min. at 95 °C, 40 cycles of 15 sec. at 95 °C and 1 min. at 60 °C. Primers were designed using the National Center for Biotechnology Primer-Blast tool (http://www.ncbi.nlm.nih.gov/tools/primer-blast/). Whenever possible, primers were designed to cross an exon junction span and designed to amplify a common region in the event of multiple splice variants. Relative mRNA expression was calculated using the $2^{-\Delta\Delta Ct}$ method using TATA-Box Binding Protein (TBP) as a normalizing gene (Livak and Schmittgen, 2001). Primers are listed in the following table.

Table 2-1: List of primers for qPCR

Gene	Forward Primer	Reverse Primer
ACHE	GGGGCTCAGCAGTACGTTAG	CGGTGGCGCTGAGCAATTT
BCHE	CTTTGTTGCAGAGAATCGGAAATC	CGGTGGCGCTGAGCAATTT
DCX	GACTCAGCAAACGGAACCTCC	GAATCACCAAGCGAGTCCGA
MAP2	TGCGCTGATTCTTCAGCTTG	TGTGTCGTGTTCTCAAAGGGT
HES5	CGGCACCAGCCCAACTCCAA	GCGACGAAGGCTTTGCTGTGC
HES1	GAAAGATAGCTCGCGGCATT	TACTTCCCCAGCACACTTGG
HES3	CTGATGGAGAAAAAGCGCCG	TTCCGGATCTGGTGCGAGTA
DELTA4	TGTGCAAGAAGCGCAATGAC	AAGACAGATAGGCTGTTGGCA
JAG1	GTCTCAACGGGGGAACTTGT	GCGTGCTCAGCAATTTCACA
SOX2	GCAATAGCATGGCGAGCG	GTTGCTCCAGCCGTTCATGT
GFAP	CATCGAGATCGCCACCTACA	GCTTTTGCCCCCTCGAATC
TBP	AAGACCATTGCACTTCGTGCCC	TGGACTGTTCTTCACTCTTGGCTCC
CYP3A7	TTGAAACACGTCTTTGGGGC	TGAGAGAACGAATGGATCTAATGGA
CYP450 Reductase	TGCCAGCGTTTCATGATCAAC	GAGACCCACGATGAGCGAAA

2.5 Butyrylcholinesterase and Acetylcholinesterase Enzyme Assays

A 96 well microplate format assay was developed from modification of the methods described previously (Richardson and Chambers, 2003). All samples and reagents were stored on ice prior to incubation at 37 °C. Frozen cell pellets were re-suspended in 200-300 µL of 50 mM Tris buffer 50 (pH 7.4 at 37 °C). Cell pellets were sonicated on ice for 20 pulses using a Labsonic®M (Sartorius Stedim Biotech) at the setting .85 cycle/75%

amplitude. Between 15-30 µg of protein (20 µL cell culture lysate) was assayed in duplicate spectrophotometrically, using 1 mM Acetylthiocholine iodide (A5751, Sigma-Aldrich) as the substrate for AChE activity and 2 mM S-Butyrylthiocholine iodide (B3253, Sigma-Aldrich) as the substrate for BChE activity. The chromagen 5,5'-dithio-bis(nitrobezoic acid) (DTNB, D218200, Sigma-Aldrich) was used at a final assay concentration of 0.3 mM, and 10 µM of eserine sulfate (E8375, Sigma-Aldrich) was used in duplicate parallel samples to correct for non-enzymatic substrate hydrolysis. All reagents were prepared in Tris buffer from stock concentrations. The microplate containing sample, chromagen and inhibitor (if required) was pre-incubated for 10 minutes at 37 °C with shaking. Substrate was then added and the microplate was immediately read kinetically at 412 nm for 20 minutes at 41 second intervals with the plate mixing function on. Specific activity was calculated as nmoles product formed per minute per mg protein using the extinction coefficient 14150 $M^{-1}cm^{-1}$, 0.56 cm path length and a 200 µl reaction volume. The protein concentration of cell lysates was measured using the Pierce BCA Protein Assay Kit (Thermo Scientific) following the microplate procedure. Both the enzyme and protein assays were performed on the SpectraMax® M5 Multi-Mode Microplate Reader (Molecular Devices).

2.6 Immunocytochemistry and Microscopy

NSCs were plated on poly-D-lysine (PDL, P0899, Sigma))/laminin (Lam, L2020, Sigma) coated 12 mm glass coverslips on Day 2 of differentiation and allowed to differentiate for 90 days. Sterile coverslips were coated with PDL/Lam in 24 well cell culture plates. Coverslips were incubated for 2 hours at 37 °C with 10 µg/mL in 0.6 M borate buffer (pH 8.5), and washed twice with sterile distilled H_2O followed by

incubation for 2 hours at 37 °C with Lam 10 µg/mL in PBS. Lam was aspirated prior to plating NSCs at a density of 400,000 cells per well. Once plated on PDL/Lam cultures were fed with differentiation media containing 1 µg/mL Lam. On Day 90, cultures were then fixed in 4% paraformaldehyde, followed by an incubation for 1 hour with 4% normal goat serum and .01% triton x-100 in PBS to permeabilize and block. Cells were then incubated at 4 °C overnight with the following antibodies: MAP2 (MAB3418, Millipore, 1:1000), Neuronal Class III β-Tubulin (TUJ1, MMS-435P, Covance, 1:2000), Synaptophysin (04-1019, Millipore, 1:500), vesicular glutamate transporter 1 (VGLUT1, 135302, Synaptic Systems, 1:500) and Glial Fibrillary Acidic Protein (GFAP, M0761, DakoCytomation, 1:1000), followed by removal of the primary antibody and triplicate PBS washes. The next day, cultures were incubated for 1 hour at room temperature with the following secondary antibodies: Alexa Fluor® 488 conjugate (A11034, Goat anti-Rabbit IgG; A21131, Goat anti-Mouse IgG2A) and Alexa Fluor® 594 conjugate (A21125, Goat anti-Mouse IgG1) at a 1:500 concentration. Nuclei were stained with DAPI (0.3 µg/ml, Roche) and rinsed well with PBS then distilled water prior to mounting. Microphotographs were taken using an Olympus 1X71 inverted microscope at 40 x objective magnification under fluorescence. In addition, live cell cultures plated on BD Matrigel™ were also photographed using phase contrast on Days 0-6.

2.7 Statistical Analysis

Experiments were performed at independent times and cell passages, and each differentiation was considered a biological replicate. To account for replicate differences, a one way ANOVA model accounting for batch variation was used to analyze changes in mRNA expression and enzyme activity. For CPS and lentivirus

treated samples, paired t tested were used for each time point to analyze expression differences between treatment and control. Data are presented as bar graphs with error bars representing mean ± standard error of mean (SEM). All statistical analysis was performed using R version 3.2.2.

3.0 RESULTS

3.1 Neural Stem Cell Model of Early Neuronal Differentiation

To establish a model of early neuronal differentiation, NSCs derived from human iPSCs were differentiated. Switching from a medium containing FGF to a medium containing BDNF reduces cell proliferation and favors differentiation (Fig 3-1a). During the six days of differentiation, cells change from a homogenous appearance to one of clustered cell bodies, with outgrowth of processes between clusters (Fig. 3-1b). After 90 days of differentiation, cells were stained for the neuronal markers including synaptophysin, Vglut, Tuj1, MAP2 and the astrocytic marker GFAP (Fig 3-1c). MAP2 co-localized with Tuj1 and synaptophysin. Vglut staining had a more punctate appearance, and indicated the presence of mainly glutamatergic neurons. Cells cultures also stain positive for GFAP, which did not co-localize with MAP2, and GFAP and MAP2 stained cells occurred in approximately equal proportion. This model showed morphological changes consistent with neurogenesis during early neuronal differentiation. At the end of 90 days, cultured were positive for neuronal markers and the astrocytic marker GFAP indicating that NSCs were differentiating into both astrocytic and neuronal lineages.

To assess early neuronal differentiation, three expression markers of NSC differentiation were selected and validated based on marked up-regulation during

differentiation (Fig.3-1d). HES5 was selected from an RNAseq data base of differentiating human ESCs. MAP2 and DCX were selected as neuronal markers that were shown to be perturbed by neurotoxicants in an ESC model of neuronal differentiation (Zimmer *et al.*, 2011). MAP2 is a cytoskeletal protein that associated with microtubules as well as a neuronal marker (Peng *et al.*, 1985). DCX is a microtubule-associated protein specific to the brain which is expressed by migrating neuroblasts during differentiation (Bai *et al.*, 2003). HES5 is a repressive transcription factor which regulates neuronal differentiation, and, along with HES1, is an effector of the Notch pathway (Kageyama and Ohtsuka, 1999). All markers showed significant upregulation on Day 4 and 6, indicating neuronal differentiation. Changes in BChE and AChE expression were also assessed (Fig. 3-2).

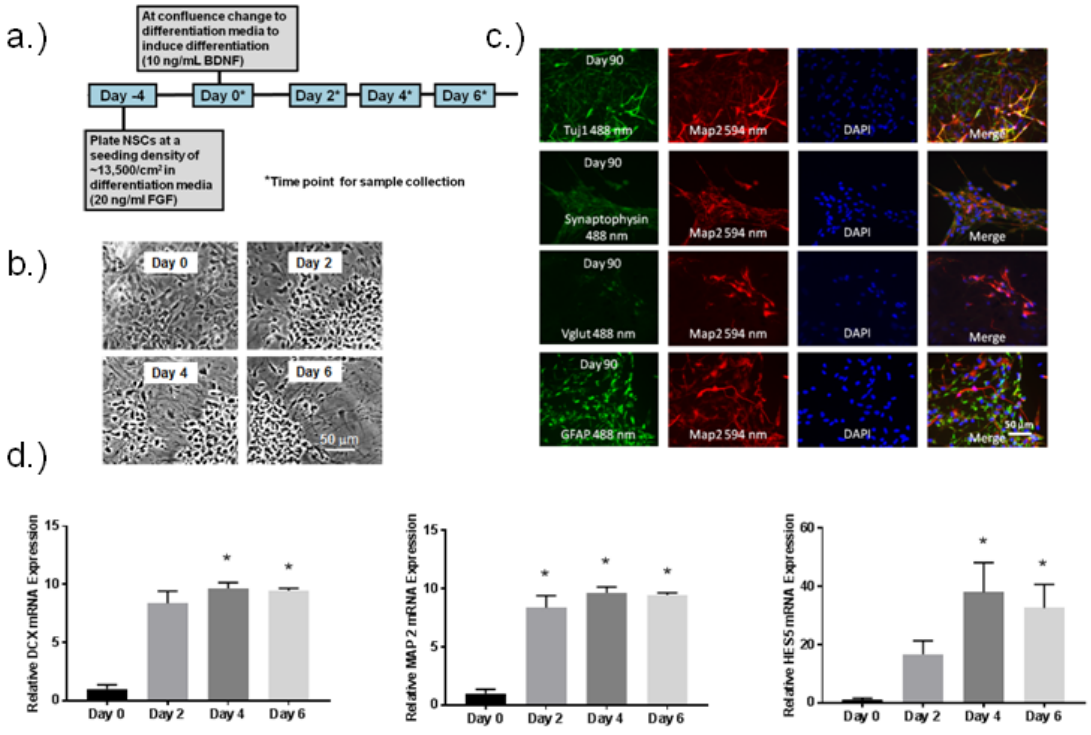

Fig. 3-1: Characterization of Neural Stem Cell model of differentiation.
a.) Overview of the experimental timeline of differentiation. **b.)** Phase-contrast microscopy showing morphological changes of NSC after induction of differentiation. **c.)** After ninety days of differentiation cultures stain positive for MAP2, Tuj1, Synaptophysin, VGlut and GFAP. **d.)** The relative mRNA expression of the differentiation markers DCX, MAP2 and HES5 were determined by quantitative real-time PCR. All three markers increased significantly relative to Day 0. Data represent mean ± SEM (n=3-5), Data was analyzed using a one-way ANOVA model to account for batch variation followed by Tukey multiple comparisons of means (* $p < 0.05$).

3.2 Butyrylcholinesterase Expression and Activity is Upregulated

To determine if AChE and BChE are expressed and regulated during early neuronal differentiation, expression and activity of both enzymes were detected using qPCR and a spectophotometric assays, respectively (Fig. 3-2). During differentiation, BChE mRNA expression and activity were significantly upregulated during the six day differentiation time course. Both activity and expression were maximally upregulated on Day 6, and BChE mRNA expression levels mirrored activity. AChE expression and activity was not significantly regulated relative to Day 0. This indicates that BChE mRNA expression

and activity is upregulated along with the expression of the other markers of differentiation (HES5, DCX and MAP2). This suggests that BChE may play a role in early differentiation of NSCs.

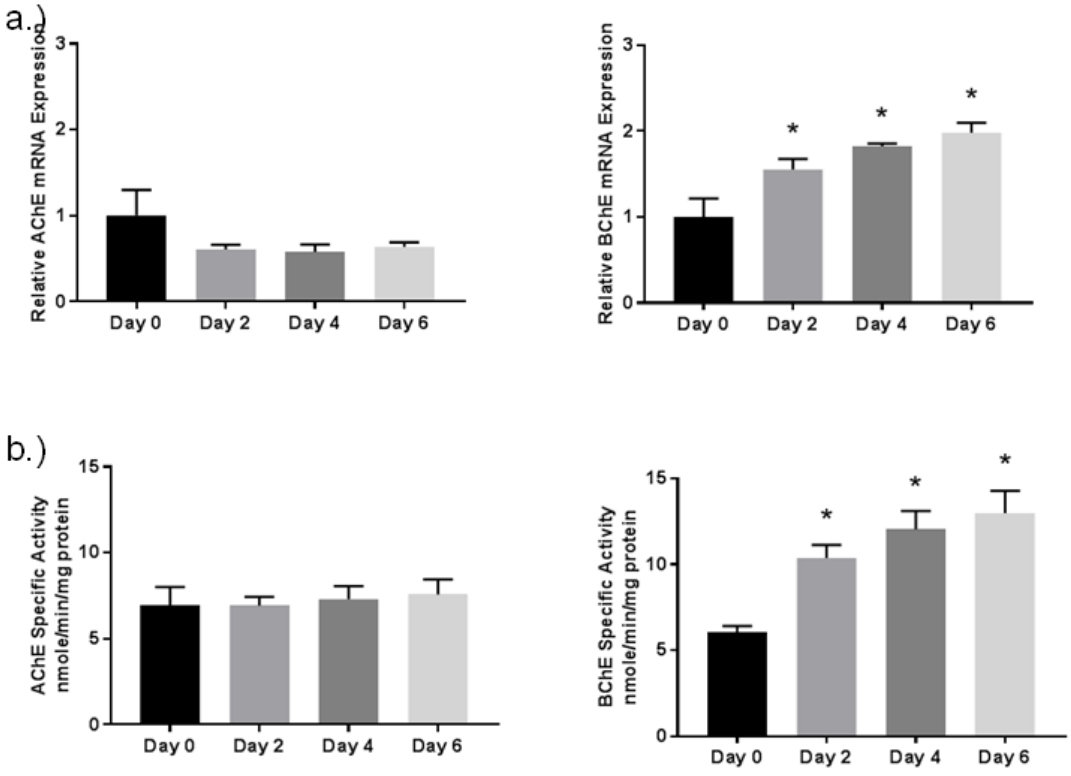

Fig. 3-2: AChE and BChE activity and expression during early neuronal differentiation. a.) The relative mRNA expression of the enzymes AChE and BChE were determined by quantitative real-time PCR. BChE mRNA expression increased significantly relative to Day 0 on all subsequent time points shown. **b.)** AChE and BChE specific activity was assayed using a kinetic spectrophotometric assay. BChE specific activity increased significantly on all subsequent time points relative to Day 0, mirroring the mRNA expression. Data represent mean ± SEM (n=5-6), Data was analyzed using a one-way ANOVA model to account for batch variation followed by Tukey multiple comparisons of means (* $p < .05$).

3.3 Cholinesterase Inhibition by Chlorpyrifos Does Not Affect Neuronal Marker Expression

To test our hypothesis that CPS inhibition of cholinesterase affects neurogenesis, NSC cultures were treated with 10 µM CPS. The 10 µM concentration did not have an

obvious effect on cell morphology, and did not change cell viability as assayed with Alamar Blue® (data not shown). CPS inhibited AChE and BChE activity 82% and 92%, respectively (Fig. 3-3a). This inhibition did not change expression of AChE or BChE mRNAs relative to control group (Fig. 3-3b). In addition, the markers of neuronal differentiation (HES5, MAP2 or DCX) were not altered by CPS treatment (Fig. 3-3c). No effect on differentiation by CPS inhibition of AChE or BChE was detected.

To assess metabolism in our model, CYP450 and CP450 reductase expression was measured by qPCR. Cultures showed expression of the enzyme CYP3A7 and CYP450 reductase during all days of differentiation, and the Ct values were approximately 31.5 and 24.5, respectively. The presence of metabolizing enzymes and cholinesterase inhibition indicates this model of neuronal differentiation can bioactivate CPS

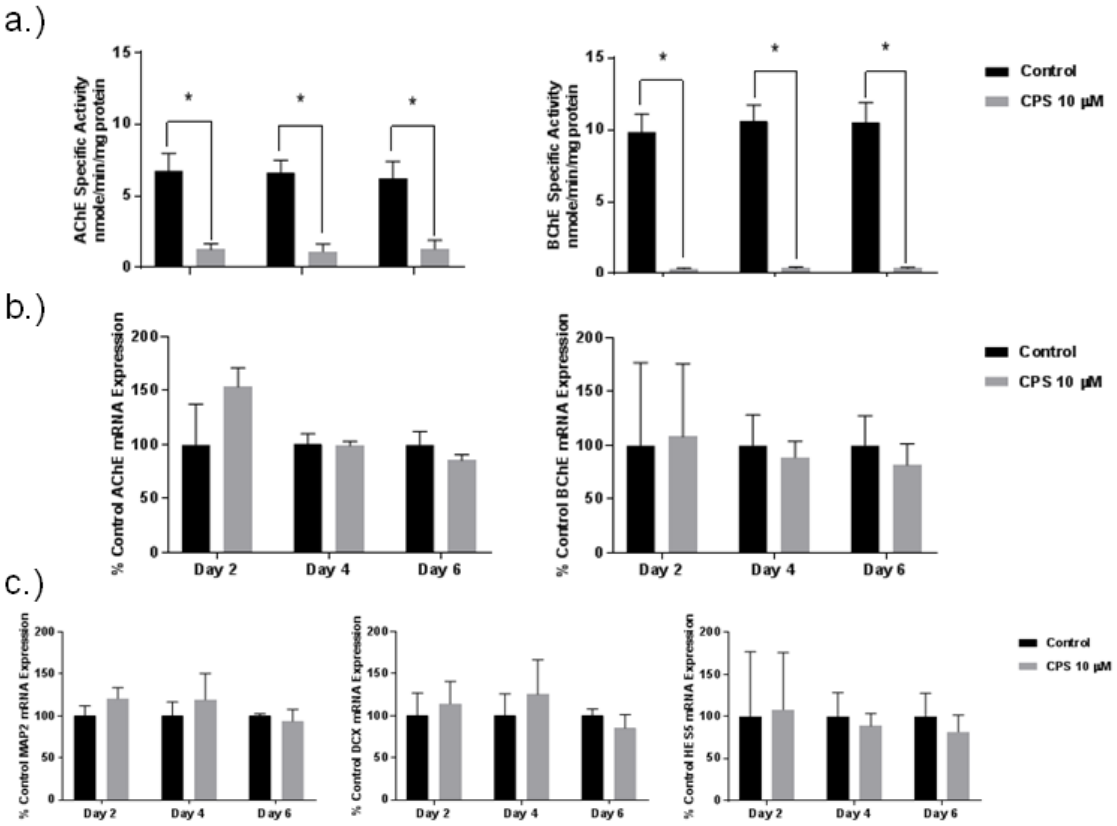

Fig. 3-3 Inhibition of AChE and BChE by CPS. Cells cultures were exposed continuously to CPS 10 µM starting on Day 0 (see Fig. 3-1a). **a.)** AChE and BChE specific activity was assayed using a kinetic spectrophotometric assay. Both AChE and BChE were inhibited, by 82% and 92% respectiviely. The relative mRNA expression of the enzymes AChE and BChE (**b.**) and the differentiation markers MAP2, DCX and HES5 (**c.**) were determined by qPCR. There were no significant differences between the control and CPS 10 µM exposure groups. Data represent mean ± SEM (n=3). Data was analyzed using paired t tests for each time point to account for batch variation. (* $p < 0.05$).

3.4 Knockdown of BChE mRNA Altered HES Gene mRNA Expression

To test our hypothesis that non-enzymatic functions of BChE regulate neurogenesis, NSCs were infected with lentivirus containing BChE or control shRNA 72 hours prior to induction of differentiation on Day 0 (Fig. 3-4a). Knockdown was assayed by qPCR on Day 0 and Day 6, and knockdown of mRNA was calculated to be 72% (Fig. 3-4b). A Western blot to confirm knockdown of BChE protein levels was inconclusive due to lack

of specific antibody detection. BChE knockdown resulted in a significant upregulation of AChE relative to control on Day 6, and a down regulation of HES5 on Day 0 (Fig 3-4c). BChE mRNA knockdown resulted in perturbed expression of the differentiation marker HES5, an effector of the Notch pathway.

Other mRNAs were assayed for changes in expression due to BChE knockdown (Fig. 3-5). Since HSE5 is regulated by the Notch pathway, we assayed the mRNA expression of other the Notch pathway genes HES1 and GFAP, and the Notch ligands JAG1 and DELTA 4. We also assayed the mRNA expression of the NSC marker SOX2 and HES3, a related transcriptional repressor. HES3 was down regulated both on Day 0 and Day 6. HES1 was down regulated on Day 0 relative to the control. Finally the notch ligand JAG1 was down regulated on Day 6. BChE mRNA knockdown, not inhibition, changed the mRNA expression of several other genes, suggesting that BChE may have a non-enzymatic role in NSC differentiation.

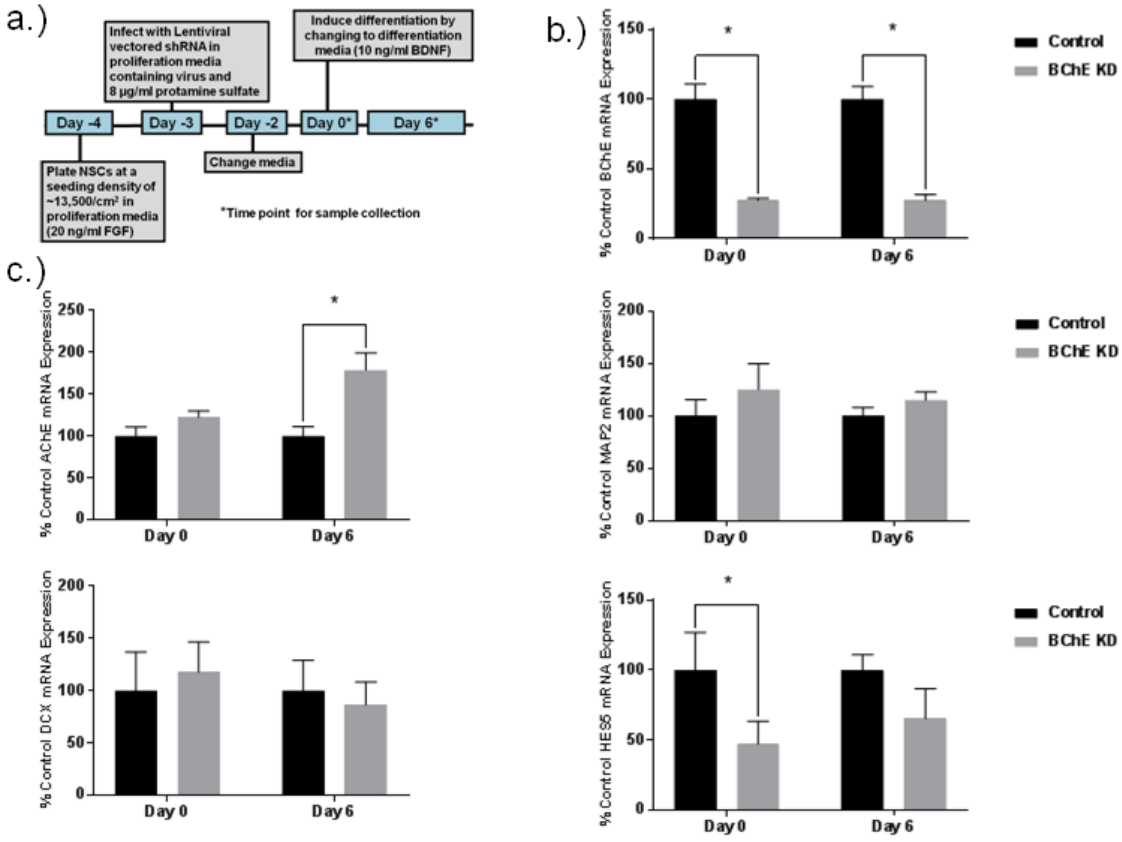

Fig. 3-4 BChE shRNA knockdown. **a.**) Overview of the experimental timeline of differentiation. **b**). BChE knockdown was calculated to be 72% by qPCR. **c.**) The relative mRNA expression of AChE the differentiation markers MAP2, DCX and HES5 were determined by qPCR. AChE expression was significantly increased on Day 6 relative to control. Only the differentiation marker HES5 was significantly decreased on Day 0 of differentiation. Data represent mean ± SEM (n=4). Data was analyzed using paired t tests for each time point to account for batch variation. (* $p < 0.05$).

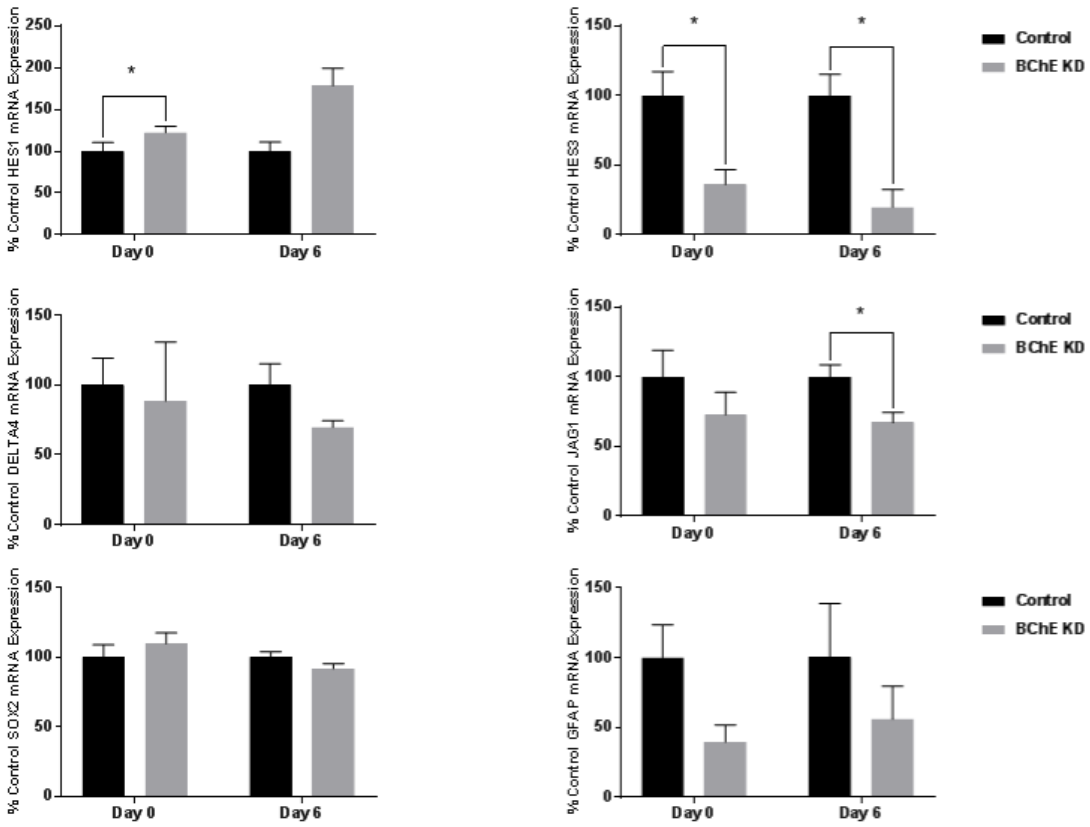

Fig. 3-5: The effect BChE knockdown on the expression of HES1, HES3, the Notch ligands DELTA4 and JAG1, SOX2 and GFAP . The relative mRNA expression of additional genes were determined by quantitative real-time PCR. HES1 was increased significantly on Day 0 relative to control, and the Notch ligand JAG1 was decreased significantly on Day 6. HES3 was decreased on both Day 0 and 6 relative to control. Data represent mean ± SEM (n=4). Data was analyzed using paired t tests for each time point to account for batch variation. (* $p < 0.05$).

4.0 DISCUSSION

In this study we use an iPSC-derived NSC model of early neuronal differentiation to probe the DNT of CPS and to assess the function of BChE in early neuronal differentiation. To assess early neuronal differentiation, three transcriptional markers were selected: HES5, DCX and MAP2. To assess the developmental toxicity of CPS through AChE and BChE inhibition, cultures were treated with a concentration sufficient to cause enzymatic inhibition during six days of differentiation. Although 10

μM CPS inhibited cholinesterase activity, the mRNA expression of transcriptional markers was unchanged. Since BChE, not AChE, was upregulated during differentiation, we hypothesized that a non-enzymatic function of BChE is involved in neurogenesis. To test this hypothesis, we used lentiviral-vectored shRNA to knock down BChE. Knockdown of BChE mRNA resulted in changes in the expression of HES1, HES3 and HES3, AChE and the Notch ligand JAG1.

Our model consists of both a proliferative phase and a differentiation phase, and differentiation is characterized by morphological changes and upregulation of the neuronal markers MAP2, DCX and the transcription factor HES5. Differentiation is induced by the withdrawal of FGF and the addition of BDNF. After 90 days of differentiation, cells stain positive MAP2 and GFAP, indicating both astrocytic and neuronal phenotypes (Fig 3-1c). In addition, cells were positive for the mature neuronal marker synaptophysin. Neurons were primarily glutamatergic and stained positive for Vglut.

As expected, this model also displayed expression of both BChE and AChE, although only BChE was mRNA and activity was increased during the six days of differentiation. BChE is known to be upregulated prior to AChE in early embryonic development, and in neural crest cells BChE is expressed during mitosis and AChE is expressed during migration and through differentiation (Layer and Sporns, 1987). This characteristic upregulation of BChE during early differentiation is consistent with the hypothesis that BChE may have a role in early neuronal differentiation.

To determine if the catalytic activity of AChE and BChE is essential for early neuronal differentiation, cells were treated continuously with a concentration of CPS

sufficient to inhibit AChE and BChE, but not enough to cause overt cytotoxicity. This concentration did not change expression of the differentiation markers, but since morphological characterization like neurite outgrowth was not performed, we cannot conclude that CPS does not effect neuronal differentiation in this model, and further study is required. In a study using NSCs derived from human umbilical cord blood to model DNT, minimal toxicity was observed at 10 µM concentration of CPS, although cells differentiated towards an astrocytic phenotype showed some decrease in viability (Buzanska *et al.*, 2009). Another recent study used a commercial human NPC line to test epigenetic effects of CPS in both proliferating and differentiating NSCs, and toxic effects were not detected at concentrations below 57 µM (Kim *et al.*, 2016). Neither studied quantified cholinesterase activity, and conversion of CPS to the active metabolite CPO is required for cholinesterase inhibition. Interestingly, we were able to detect mRNA expression of both the CYP3A7 and CYP450 reductase in our stem cell model. CYP3A7, a fetal enzyme, has been shown to covert CPS to the active oxon at low micromolar concentrations of CPS (Buratti *et al.*, 2006). An *in vitro* model does not adequately recapitulate all aspects of *in vivo* neuronal differentiation. Many endpoints of CPS DNT modeled *in vitro* are at concentrations high enough to cause AChE inhibition or even overt signs of cholinergic toxicity *in vivo* (Buzanska *et al.*, 2009; Kim *et al.*, 2016; Slotkin and Seidler, 2012; Slotkin *et al.*, 2008). Although *in vitro* models may not be sensitive enough to screen some developmental neurotoxicants at doses relevant to those expected from low, chronic environmental exposure, they are a valuable tool to probe the mechanisms underlying neurogenesis and DNT.

To test the hypothesis that BChE is required for neuronal differentiation of NSCs, we used lentiviral vectored shRNA to generate a stable knockdown of BChE mRNA and

protein, although knockdown of protein was not confirmed. BChE knockdown changed the reduced expression of our pre-selected marker of differentiation HES5 by over 50%. BChE knockdown caused changes in the expression of other genes known to be involved in early neuronal differentiation including AChE, HES3, HES1 and JAG1, but knockdown did not change expression of neuronal markers MAP2, DCX or the astrocytic marker GFAP. On Day 0 after BChE knockdown, prior to differentiation, HES1, HES3 and HES5 mRNA expression were found to be statistically different than the control, suggesting that BChE expression is involved in HES signaling.

The repressor-type basic helix-loop-helix (bHLH) genes HES1, HES3 and HES5 play a critical role in NSC differentiation and maintenance (Kageyama *et al.*, 2005). Activating bHLH genes including Mash1, Math and Neurogenin promote neurogenesis, where as the repressor bHLH genes promote gliogenesis, which are formed later in neural stem cell differentiation. Only HES1 and HES5 are regulated by the Notch pathway (Ohtsuka *et al.*, 1999). HES3 is not regulated by the Notch pathway (Nishimura *et al.*, 1998). HES1 and HES5 can functionally compensate for each other, although HES1/HES5 double knockout mice show decreased maintenance of glial cells and increased early neurogenesis (Kageyama *et al.*, 2005). Triple knockout HES1/HES3/HES5 mice have a more severe phenotype, which results in premature differentiation of stem cells in neurons, and a loss of other cell type including astrocytes and oligodendrocytes (Hatakeyama *et al.*, 2004).

We have shown that HES expression in NSCs was perturbed after BChE knockdown. On Day 0, HES5 expression was down regulated and HES1 was upregulated. HES3 expression was down regulated on both Day 0 and Day 6, and the Notch ligand JAG1 was upregulated only on Day 6. Although HES expression is altered, there is no change

in expression of the neuronal markers DCX and MAP2 or the astrocytic marker GFAP. HES1 upregulation may have compensated for HES3/HES5 down regulation. Alternatively, differences in neuronal and glial mRNA expression may have been significantly different at a later time point of differentiation. Although this study is limited by only mRNA expression differences found in five of the ten genes assayed and lack of protein expression, the result support the hypothesis that BChE may have a novel role in the maintenance and differentiation of NSCs, possible through a non-enzymatic mechanism.

In our stem cell model, AChE mRNA was increased by approximately 75% on Day 6 after BChE knockdown. This is not completely unexpected, as AChE has been shown to be counter regulated with BChE in R28 rat retinal cell line through the transcription factors P90RSK1 and c-fos, and siRNA knockdown of BChE resulted in "drastically increased" AChE mRNA and protein expression (Bodur and Layer, 2011). Although AChE was upregulated after BChE knockdown in our model (Fig. 3-4), AChE mRNA expression and activity did not appear to be down regulated during early differentiation when BChE expression and activity increased (Fig. 3-2). AChE is considered more likely than BChE to have a non-enzymatic role in neurogenesis (Johnson and Moore, 2012), and changes in AChE expression cannot be ruled out as the cause of mRNA expression changes.

AChE may interact with other proteins during neurogenesis through the peripheral anionic site. There is a greater concentration of negative electrostatic charge on the peripheral anionic site of AChE compared to BChE (Felder *et al.*, 1997). AChE has been shown to participate in protein:protein interactions via the peripheral anionic site with basement membrane molecules (Johnson and Moore, 2003), and amyloid β in

Alzheimer's disease (Inestrosa *et al.*, 2008). Both AChE and BChE knockout mice exist, but neither has major neurological malformations. The AChE knockout mouse does have defects in retinal structure (Mesulam *et al.*, 2002), where as the BChE knockout has a near normal phenotype (Li *et al.*, 2006). In humans, various mutations result in decreased BChE activity, but it is unclear if any of these result in the complete absence of BChE protein or mRNA (Johnson and Moore, 2012). A recent paper described reduced fibrillar β-amyloid in an BChE-knockout Alzheimer disease mouse model (Darvesh and Reid, 2016), and the underlying mechanism is suggested to be through a non-enzymatic interaction of β-amyloid with residues of BChE found at the lip of the active site gorge (Kumar *et al.*, 2016).

We propose BChE may interact with other proteins during NSC differentiation through a non-enzymatic mechanism. Since HES5 expression was decreased with BChE knockdown, Notch pathway proteins are a speculative candidate. Notch is activated by ligands and cleaved by intercellular γ-Secretase. After cleavage, the Notch intracellular domain translocates to the nucleus where it binds to the HES1 and HES5 promotor and upregulates expression (Kageyama and Ohtsuka, 1999), although in some case Notch may decrease HES5 expression. Notch does not regulate HES3 expression, so the changes in gene expression cause by BChE knockdown may be a symptom of a more global transcriptional perturbation. The notch ligand JAG1 was decreased on Day 6 of differentiation. JAG1 is involved postnatal and adult neurogenesis in the dentate gyrus (Lavado and Oliver, 2014), and astrocytes have been shown to decrease neurogenesis though Notch/JAG1 signaling (Wilhelmsson *et al.*, 2012). Further studies profiling transcriptional changes in the of genes known to be involved in neuronal differentiation, as well as a confirmation of protein expression changes would give a more complete

picture as to the mechanism underlying the non-enzymatic role of BChE in NSC differentiation. Assessing changes in viability with BChE knockdown would also be informative, as BChE is thought to have a role in proliferation (Robitzki *et al.*, 1997). Quantifying neuronal and astrocytic cells at later time points of differentiation would indicate if BChE knockdown results in changes in cell fate determination. Finally, demonstrating interaction of BChE with a putative target in neuronal differentiation would show the underlying molecular interaction.

BChE is an enigmatic protein. It functions in xenobiotic metabolism, cholinergic signaling and, in addition, may have a role in embryonic neurogenesis. AChE shows structural and functional homology with BChE, and the coordinated expression of these two enzymes early on in embryogenesis indicate a functional redundancy. A non-enzymatic role of BChE through regulation of HES genes or Notch is a novel mechanism through which the cholinesterases may function in neurogenesis.

5.0 REFERENCES

Alles, G. A., and Hawes, R. C. (1940). CHOLINESTERASES IN THE BLOOD OF MAN. *J. Biol. Chem.* **133**(2), 375-390.

Bai, J., Ramos, R. L., Ackman, J. B., Thomas, A. M., Lee, R. V., and LoTurco, J. J. (2003). RNAi reveals doublecortin is required for radial migration in rat neocortex. *Nat. Neurosci.* **6**(12), 1277-83.

Bear, M. F., Connors, B. W., and Paradiso, M. A. (2007). *Neuroscience : exploring the brain*. 3rd ed. Lippincott Williams & Wilkins, Philadelphia, PA.

Berkowitz, G. S., Wetmur, J. G., Birman-Deych, E., Obel, J., Lapinski, R. H., Godbold, J. H., Holzman, I. R., and Wolff, M. S. (2004). In utero pesticide exposure, maternal paraoxonase activity, and head circumference. *Environ. Health Perspect.* **112**(3), 388-91.

Blondet, B., Carpentier, G., Ferry, A., Chatonnet, A., and Courty, J. (2010). Localization of butyrylcholinesterase at the neuromuscular junction of normal and acetylcholinesterase knockout mice. *J. Histochem. Cytochem.* **58**(12), 1075-82.

Bodur, E., and Layer, P. G. (2011). Counter-regulation of cholinesterases: differential activation of PKC and ERK signaling in retinal cells through BChE knockdown. *Biochimie* **93**(3), 469-76.

Bradley, A., Evans, M., Kaufman, M. H., and Robertson, E. (1984). Formation of germ-line chimaeras from embryo-derived teratocarcinoma cell lines. *Nature* **309**(5965), 255-6.

Brazzolotto, X., Wandhammer, M., Ronco, C., Trovaslet, M., Jean, L., Lockridge, O., Renard, P. Y., and Nachon, F. (2012). Human butyrylcholinesterase produced in insect cells: huprine-based affinity purification and crystal structure. *FEBS J.* **279**(16), 2905-16.

Briggs, R., and King, T. J. (1952). Transplantation of Living Nuclei From Blastula Cells into Enucleated Frogs' Eggs. *Proc. Natl. Acad. Sci. U. S. A.* **38**(5), 455-63.

Brinster, R. L. (1974). The effect of cells transferred into the mouse blastocyst on subsequent development. *J. Exp. Med.* **140**(4), 1049-56.

Buratti, F. M., Leoni, C., and Testai, E. (2006). Foetal and adult human CYP3A isoforms in the bioactivation of organophosphorothionate insecticides. *Toxicol. Lett.* **167**(3), 245-55.

Buzanska, L., Sypecka, J., Nerini-Molteni, S., Compagnoni, A., Hogberg, H. T., del Torchio, R., Domanska-Janik, K., Zimmer, J., and Coecke, S. (2009). A human stem cell-based model for identifying adverse effects of organic and inorganic chemicals on the developing nervous system. *Stem Cells* **27**(10), 2591-601.

Campanha, H. M., Carvalho, F., and Schlosser, P. M. (2014). Active and peripheral anionic sites of acetylcholinesterase have differential modulation effects on cell proliferation, adhesion and neuritogenesis in the NG108-15 cell line. *Toxicol. Lett.* **230**(2), 122-31.

Chambers, J., and Oppenheimer, S. F. (2004). Organophosphates, serine esterase inhibition, and modeling of organophosphate toxicity. *Toxicol. Sci.* **77**(2), 185-7.

Chatonnet, A., and Lockridge, O. (1989). Comparison of butyrylcholinesterase and acetylcholinesterase. *Biochem. J.* **260**(3), 625-34.

Chen, X. P., Jin, J. L., Li, C. W., and Wang, F. S. (2009). [Effects of low concentration of chlorpyrifos prenatal exposure on generation mouse brain hippocampus and somatosensory cortex]. *Zhonghua Lao Dong Wei Sheng Zhi Ye Bing Za Zhi* **27**(9), 557-9.

Costa, L. G. (2008). Toxic effects of pesticides. In *Casarett and Doull's Toxicology: The Basic Science of Poisons* (C. D. Klaassen, Eds.) doi, pp. 883-930. McGraw-Hill Medical, New York.

Costa, L. G., Giordano, G., Guizzetti, M., and Vitalone, A. (2008). Neurotoxicity of pesticides: a brief review. *Front. Biosci.* **13**, 1240-9.

Cowan, C. A., Atienza, J., Melton, D. A., and Eggan, K. (2005). Nuclear reprogramming of somatic cells after fusion with human embryonic stem cells. *Science* **309**(5739), 1369-73.

Crane, A. L., Klein, K., Zanger, U. M., and Olson, J. R. (2012). Effect of CYP2B6*6 and CYP2C19*2 genotype on chlorpyrifos metabolism. *Toxicology* **293**(1-3), 115-22.

Darvesh, S., Grantham, D. L., and Hopkins, D. A. (1998). Distribution of butyrylcholinesterase in the human amygdala and hippocampal formation. *J. Comp. Neurol.* **393**(3), 374-90.

Darvesh, S., Hopkins, D. A., and Geula, C. (2003). Neurobiology of butyrylcholinesterase. *Nat. Rev. Neurosci.* **4**(2), 131-8.

Darvesh, S., and Reid, G. A. (2016). Reduced fibrillar beta-amyloid in subcortical structures in a butyrylcholinesterase-knockout Alzheimer disease mouse model. *Chem Biol Interact* doi: 10.1016/j.cbi.2016.04.022, 10.1016/j.cbi.2016.04.022.

Drews, U. (1975). Cholinesterase in embryonic development. *Prog. Histochem. Cytochem.* **7**(3), 1-52.

Eaton, D. L., Daroff, R. B., Autrup, H., Bridges, J., Buffler, P., Costa, L. G., Coyle, J., McKhann, G., Mobley, W. C., Nadel, L., Neubert, D., Schulte-Hermann, R., and Spencer, P. S. (2008). Review of the toxicology of chlorpyrifos with an emphasis on human exposure and neurodevelopment. *Crit. Rev. Toxicol.* **38 Suppl 2**, 1-125.

EPA (2014). Revised Human Health Risk Assessment on Chlorpyrifos.

Evans, M. J., and Kaufman, M. H. (1981). Establishment in culture of pluripotential cells from mouse embryos. *Nature* **292**(5819), 154-6.

Felder, C. E., Botti, S. A., Lifson, S., Silman, I., and Sussman, J. L. (1997). External and internal electrostatic potentials of cholinesterase models. *J Mol Graph Model* **15**(5), 318-27, 335-7.

Gatley, S. J. (1991). Activities of the enantiomers of cocaine and some related compounds as substrates and inhibitors of plasma butyrylcholinesterase. *Biochem. Pharmacol.* **41**(8), 1249-54.

Gerrard, L., Rodgers, L., and Cui, W. (2005). Differentiation of human embryonic stem cells to neural lineages in adherent culture by blocking bone morphogenetic protein signaling. *Stem Cells* **23**(9), 1234-41.

Goff, L. A., Davila, J., Swerdel, M. R., Moore, J. C., Cohen, R. I., Wu, H., Sun, Y. E., and Hart, R. P. (2009). Ago2 immunoprecipitation identifies predicted microRNAs in human embryonic stem cells and neural precursors. *PLoS One* **4**(9), e7192, 10.1371/journal.pone.0007192.

Grigoryan, H., and Lockridge, O. (2009). Nanoimages show disruption of tubulin polymerization by chlorpyrifos oxon: implications for neurotoxicity. *Toxicol. Appl. Pharmacol.* **240**(2), 143-8.

Gunier, R. B., Bradman, A., Harley, K. G., Kogut, K., and Eskenazi, B. (2016). Prenatal Residential Proximity to Agricultural Pesticide Use and IQ in 7-Year-Old Children. *Environ. Health Perspect.* doi: 10.1289/ehp504, 10.1289/ehp504.

Gurdon, J. B., Elsdale, T. R., and Fischberg, M. (1958). Sexually mature individuals of Xenopus laevis from the transplantation of single somatic nuclei. *Nature* **182**(4627), 64-5.

Hatakeyama, J., Bessho, Y., Katoh, K., Ookawara, S., Fujioka, M., Guillemot, F., and Kageyama, R. (2004). Hes genes regulate size, shape and histogenesis of the nervous system by control of the timing of neural stem cell differentiation. *Development* **131**(22), 5539-50.

He, F., Xu, H., Qin, F., Xu, L., Huang, J., and He, X. (1998). Intermediate myasthenia syndrome following acute organophosphates poisoning--an analysis of 21 cases. *Hum. Exp. Toxicol.* **17**(1), 40-5.

Holmquist, M. (2000). Alpha/Beta-hydrolase fold enzymes: structures, functions and mechanisms. *Curr Protein Pept Sci* **1**(2), 209-35.

Ichikawa, T., Ajiki, K., Matsuura, J., and Misawa, H. (1997). Localization of two cholinergic markers, choline acetyltransferase and vesicular acetylcholine transporter in the central nervous system of the rat: in situ hybridization histochemistry and immunohistochemistry. *J. Chem. Neuroanat.* **13**(1), 23-39.

Inestrosa, N. C., Dinamarca, M. C., and Alvarez, A. (2008). Amyloid-cholinesterase interactions. Implications for Alzheimer's disease. *FEBS J.* **275**(4), 625-32.

Jbilo, O., Bartels, C. F., Chatonnet, A., Toutant, J. P., and Lockridge, O. (1994). Tissue distribution of human acetylcholinesterase and butyrylcholinesterase messenger RNA. *Toxicon* **32**(11), 1445-57.

Johnson, G., and Moore, S. W. (2003). Human acetylcholinesterase binds to mouse laminin-1 and human collagen IV by an electrostatic mechanism at the peripheral anionic site. *Neurosci. Lett.* **337**(1), 37-40.

Johnson, G., and Moore, S. W. (2012). Why has butyrylcholinesterase been retained? Structural and functional diversification in a duplicated gene. *Neurochem. Int.* **61**(5), 783-97.

Kageyama, R., and Ohtsuka, T. (1999). The Notch-Hes pathway in mammalian neural development. *Cell Res.* **9**(3), 179-88.

Kageyama, R., Ohtsuka, T., Hatakeyama, J., and Ohsawa, R. (2005). Roles of bHLH genes in neural stem cell differentiation. *Exp. Cell Res.* **306**(2), 343-8.

Kelly, S. J. (1977). Studies of the developmental potential of 4- and 8-cell stage mouse blastomeres. *J. Exp. Zool.* **200**(3), 365-376.

Khokhar, J. Y., and Tyndale, R. F. (2012). Rat brain CYP2B-enzymatic activation of chlorpyrifos to the oxon mediates cholinergic neurotoxicity. *Toxicol. Sci.* **126**(2), 325-35.

Kim, H. Y., Wegner, S. H., Van Ness, K. P., Park, J. J., Pacheco, S. E., Workman, T., Hong, S., Griffith, W., and Faustman, E. M. (2016). Differential epigenetic effects of chlorpyrifos

and arsenic in proliferating and differentiating human neural progenitor cells. *Reprod. Toxicol.* **65**, 212-223.

Kleinsmith, L. J., and Pierce, G. B., Jr. (1964). MULTIPOTENTIALITY OF SINGLE EMBRYONAL CARCINOMA CELLS. *Cancer Res.* **24**, 1544-51.

Kumar, R., Nordberg, A., and Darreh-Shori, T. (2016). Amyloid-beta peptides act as allosteric modulators of cholinergic signalling through formation of soluble BAbetaACs. *Brain* **139**(Pt 1), 174-92.

Lavado, A., and Oliver, G. (2014). Jagged1 is necessary for postnatal and adult neurogenesis in the dentate gyrus. *Dev. Biol.* **388**(1), 11-21.

Layer, P. G., Klaczinski, J., Salfelder, A., Sperling, L. E., Thangaraj, G., Tuschl, C., and Vogel-Hopker, A. (2013). Cholinesterases in development: AChE as a firewall to inhibit cell proliferation and support differentiation. *Chem Biol Interact* **203**(1), 269-76, 10.1016/j.cbi.2012.09.014.

Layer, P. G., and Sporns, O. (1987). Spatiotemporal relationship of embryonic cholinesterases with cell proliferation in chicken brain and eye. *Proc. Natl. Acad. Sci. U. S. A.* **84**(1), 284-8.

Layer, P. G., and Willbold, E. (1995). Novel functions of cholinesterases in development, physiology and disease. *Prog. Histochem. Cytochem.* **29**(3), 1-94.

Levin, E. D., Addy, N., Baruah, A., Elias, A., Christopher, N. C., Seidler, F. J., and Slotkin, T. A. (2002). Prenatal chlorpyrifos exposure in rats causes persistent behavioral alterations. *Neurotoxicol. Teratol.* **24**(6), 733-41.

Li, B., Duysen, E. G., Saunders, T. L., and Lockridge, O. (2006). Production of the butyrylcholinesterase knockout mouse. *J. Mol. Neurosci.* **30**(1-2), 193-5.

Li, Y., Camp, S., Rachinsky, T. L., Getman, D., and Taylor, P. (1991). Gene structure of mammalian acetylcholinesterase. Alternative exons dictate tissue-specific expression. *J. Biol. Chem.* **266**(34), 23083-90.

Liu, J., Olivier, K., and Pope, C. N. (1999). Comparative neurochemical effects of repeated methyl parathion or chlorpyrifos exposures in neonatal and adult rats. *Toxicol. Appl. Pharmacol.* **158**(2), 186-96.

Livak, K. J., and Schmittgen, T. D. (2001). Analysis of relative gene expression data using real-time quantitative PCR and the 2(-Delta Delta C(T)) Method. *Methods* **25**(4), 402-8.

Loewi, O. (1921). Über humorale übertragbarkeit der Herznervenwirkung. *Pflüger's Archiv für die gesamte Physiologie des Menschen und der Tiere* **189**(1), 239-242.

Lotti, M., and Moretto, A. (2005). Organophosphate-induced delayed polyneuropathy. *Toxicol. Rev.* **24**(1), 37-49.

Ludwig, T. E., Bergendahl, V., Levenstein, M. E., Yu, J., Probasco, M. D., and Thomson, J. A. (2006). Feeder-independent culture of human embryonic stem cells. *Nat. Methods* **3**(8), 637-46.

Mack, A., and Robitzki, A. (2000). The key role of butyrylcholinesterase during neurogenesis and neural disorders: an antisense-5'butyrylcholinesterase-DNA study. *Prog. Neurobiol.* **60**(6), 607-28.

Masson, P., Xie, W., Froment, M. T., Levitsky, V., Fortier, P. L., Albaret, C., and Lockridge, O. (1999). Interaction between the peripheral site residues of human butyrylcholinesterase, D70 and Y332, in binding and hydrolysis of substrates. *Biochim. Biophys. Acta* **1433**(1-2), 281-93.

Massoulie, J. (2002). The origin of the molecular diversity and functional anchoring of cholinesterases. *Neurosignals* **11**(3), 130-43, 65054.

McCollister, S. B., Kociba, R. J., Humiston, C. G., and McCollister, D. D. (1974). Studies on the acute and long-term oral toxicity fo chlorpyrifos (0,0-diethyl-0(3,5,6-trichloro-2-pyridyl) phosphorothioate). *Food Cosmet. Toxicol.* **12**(1), 45-61.

Mendel, B., and Hawkins, R. D. (1943). Removal of acetylcholine by cholinesterase injections and the effect thereof on nerve impulse transmission. *J. Neurophysiol.* **6**(5), 431-438.

Mendel, B., and Mundell, D. B. (1943). Studies on cholinesterase: 2. A method for the purification of a pseudo-cholinesterase from dog pancreas. *Biochem. J.* **37**(1), 64-6.

Mendel, B., Mundell, D. B., and Rudney, H. (1943). Studies on cholinesterase: 3. Specific tests for true cholinesterase and pseudo-cholinesterase. *Biochem. J.* **37**(4), 473-476. First published on 1943.

Mendel, B., and Rudney, H. (1943a). On the type of cholinesterase present in brain tissue. *Science* **98**(2539), 201-2.

Mendel, B., and Rudney, H. (1943c). Studies on cholinesterase: 1. Cholinesterase and pseudo-cholinesterase. *Biochem. J.* **37**(1), 59-63.

Meshorer, E., and Soreq, H. (2006). Virtues and woes of AChE alternative splicing in stress-related neuropathologies. *Trends Neurosci.* **29**(4), 216-24.

Mesulam, M. M., Guillozet, A., Shaw, P., Levey, A., Duysen, E. G., and Lockridge, O. (2002). Acetylcholinesterase knockouts establish central cholinergic pathways and can use butyrylcholinesterase to hydrolyze acetylcholine. *Neuroscience* **110**(4), 627-39.

Millard, C. B., and Broomfield, C. A. (1992). A computer model of glycosylated human butyrylcholinesterase. *Biochem. Biophys. Res. Commun.* **189**(3), 1280-6.

Nelakanti, R. V., Kooreman, N. G., and Wu, J. C. (2015). Teratoma formation: a tool for monitoring pluripotency in stem cell research. *Curr. Protoc. Stem Cell Biol.* **32**, 4A 8 1-17.

Nishimura, M., Isaka, F., Ishibashi, M., Tomita, K., Tsuda, H., Nakanishi, S., and Kageyama, R. (1998). Structure, chromosomal locus, and promoter of mouse Hes2 gene, a homologue of Drosophila hairy and Enhancer of split. *Genomics* **49**(1), 69-75.

O'Rahilly, R., and Muller, F. (1994). Neurulation in the normal human embryo. *Ciba Found. Symp.* **181**, 70-82; discussion 82-9.

Ohtsuka, T., Ishibashi, M., Gradwohl, G., Nakanishi, S., Guillemot, F., and Kageyama, R. (1999). Hes1 and Hes5 as notch effectors in mammalian neuronal differentiation. *EMBO J.* **18**(8), 2196-207.

Ozair, M. Z., Kintner, C., and Brivanlou, A. H. (2013). Neural induction and early patterning in vertebrates. *Wiley Interdiscip Rev Dev Biol* **2**(4), 479-98.

Paraoanu, L. E., and Layer, P. G. (2008). Acetylcholinesterase in cell adhesion, neurite growth and network formation. *FEBS J.* **275**(4), 618-24.

Pedrosa, E., Sandler, V., Shah, A., Carroll, R., Chang, C., Rockowitz, S., Guo, X., Zheng, D., and Lachman, H. M. (2011). Development of patient-specific neurons in schizophrenia using induced pluripotent stem cells. *J. Neurogenet.* **25**(3), 88-103.

Peng, I., Binder, L. I., and Black, M. M. (1985). Cultured neurons contain a variety of microtubule-associated proteins. *Brain Res.* **361**(1-2), 200-11.

Peter, J. V., Sudarsan, T. I., and Moran, J. L. (2014). Clinical features of organophosphate poisoning: A review of different classification systems and approaches. *Indian J. Crit. Care Med.* **18**(11), 735-45.

Rauh, V., Arunajadai, S., Horton, M., Perera, F., Hoepner, L., Barr, D. B., and Whyatt, R. (2011). Seven-year neurodevelopmental scores and prenatal exposure to chlorpyrifos, a common agricultural pesticide. *Environ. Health Perspect.* **119**(8), 1196-201.

Rauh, V. A., Perera, F. P., Horton, M. K., Whyatt, R. M., Bansal, R., Hao, X., Liu, J., Barr, D. B., Slotkin, T. A., and Peterson, B. S. (2012). Brain anomalies in children exposed prenatally to a common organophosphate pesticide. *Proc. Natl. Acad. Sci. U. S. A.* **109**(20), 7871-6.

Reichardt, L. F. (2006). Neurotrophin-regulated signalling pathways. *Philos. Trans. R. Soc. Lond. B Biol. Sci.* **361**(1473), 1545-64.

Richardson, J., and Chambers, J. (2003). Effects of gestational exposure to chlorpyrifos on postnatal central and peripheral cholinergic neurochemistry. *J. Toxicol. Environ. Health A* **66**(3), 275-89.

Rippon, H. J., and Bishop, A. E. (2004). Embryonic stem cells. *Cell Prolif.* **37**(1), 23-34.

Robitzki, A., Doll, F., Richter-Landsberg, C., and Layer, P. G. (2000). Regulation of the rat oligodendroglia cell line OLN-93 by antisense transfection of butyrylcholinesterase. *Glia* **31**(3), 195-205.

Robitzki, A., Mack, A., Chatonnet, A., and Layer, P. G. (1997). Transfection of reaggregating embryonic chicken retinal cells with an antisense 5'-DNA butyrylcholinesterase expression vector inhibits proliferation and alters morphogenesis. *J. Neurochem.* **69**(2), 823-33.

Roy, T. S., Sharma, V., Seidler, F. J., and Slotkin, T. A. (2005). Quantitative morphological assessment reveals neuronal and glial deficits in hippocampus after a brief subtoxic exposure to chlorpyrifos in neonatal rats. *Brain Res. Dev. Brain Res.* **155**(1), 71-80.

Saxena, A., Redman, A. M., Jiang, X., Lockridge, O., and Doctor, B. P. (1999). Differences in active-site gorge dimensions of cholinesterases revealed by binding of inhibitors to human butyrylcholinesterase. *Chem Biol Interact* **119-120**, 61-9.

Scholl, F. G., and Scheiffele, P. (2003). Making connections: cholinesterase-domain proteins in the CNS. *Trends Neurosci.* **26**(11), 618-24.

Shepherd, G. M. (1994). *Neurobiology*. 3rd ed. Oxford University Press, New York.

Slotkin, T. A., and Seidler, F. J. (2012). Developmental neurotoxicity of organophosphates targets cell cycle and apoptosis, revealed by transcriptional profiles in vivo and in vitro. *Neurotoxicol. Teratol.* **34**(2), 232-41.

Slotkin, T. A., Seidler, F. J., and Fumagalli, F. (2008). Targeting of neurotrophic factors, their receptors, and signaling pathways in the developmental neurotoxicity of organophosphates in vivo and in vitro. *Brain Res. Bull.* **76**(4), 424-38.

Stedman, E., Stedman, E., and Easson, L. H. (1932). Choline-esterase. An enzyme present in the blood-serum of the horse. *Biochem. J.* **26**(6), 2056-66.

Tada, M., Takahama, Y., Abe, K., Nakatsuji, N., and Tada, T. (2001). Nuclear reprogramming of somatic cells by in vitro hybridization with ES cells. *Curr. Biol.* **11**(19), 1553-8.

Takahashi, K., Tanabe, K., Ohnuki, M., Narita, M., Ichisaka, T., Tomoda, K., and Yamanaka, S. (2007). Induction of pluripotent stem cells from adult human fibroblasts by defined factors. *Cell* **131**(5), 861-72.

Takahashi, K., and Yamanaka, S. (2006). Induction of pluripotent stem cells from mouse embryonic and adult fibroblast cultures by defined factors. *Cell* **126**(4), 663-76.

Thomson, J. A., Itskovitz-Eldor, J., Shapiro, S. S., Waknitz, M. A., Swiergiel, J. J., Marshall, V. S., and Jones, J. M. (1998). Embryonic stem cell lines derived from human blastocysts. *Science* **282**(5391), 1145-7.

Vellom, D. C., Radic, Z., Li, Y., Pickering, N. A., Camp, S., and Taylor, P. (1993). Amino acid residues controlling acetylcholinesterase and butyrylcholinesterase specificity. *Biochemistry* **32**(1), 12-7.

Vogel-Hopker, A., Sperling, L. E., and Layer, P. G. (2012). Co-opting functions of cholinesterases in neural, limb and stem cell development. *Protein Pept Lett* **19**(2), 155-64.

Wakid, N. W., Tubbeh, R., and Baraka, A. (1985). Assay of serum cholinesterase with succinylcholine and propionylthiocholine as substrates. *Anesthesiology* **62**(4), 509-12.

Whittaker, V. P. (2010). How the cholinesterases got their modern names. *Chem Biol Interact* **187**(1-3), 23-6.

Wilhelmsson, U., Faiz, M., de Pablo, Y., Sjoqvist, M., Andersson, D., Widestrand, A., Potokar, M., Stenovec, M., Smith, P. L., Shinjyo, N., Pekny, T., Zorec, R., Stahlberg, A., Pekna, M., Sahlgren, C., and Pekny, M. (2012). Astrocytes negatively regulate neurogenesis through the Jagged1-mediated Notch pathway. *Stem Cells* **30**(10), 2320-9.

Wilmut, I., Schnieke, A. E., McWhir, J., Kind, A. J., and Campbell, K. H. (2007). Viable offspring derived from fetal and adult mammalian cells. *Cloning Stem Cells* **9**(1), 3-7.

Yang, D., Howard, A., Bruun, D., Ajua-Alemanj, M., Pickart, C., and Lein, P. J. (2008). Chlorpyrifos and chlorpyrifos-oxon inhibit axonal growth by interfering with the morphogenic activity of acetylcholinesterase. *Toxicol. Appl. Pharmacol.* **228**(1), 32-41.

Yao, S., Chen, S., Clark, J., Hao, E., Beattie, G. M., Hayek, A., and Ding, S. (2006). Long-term self-renewal and directed differentiation of human embryonic stem cells in chemically defined conditions. *Proc. Natl. Acad. Sci. U. S. A.* **103**(18), 6907-12.

Ying, Q. L., Stavridis, M., Griffiths, D., Li, M., and Smith, A. (2003). Conversion of embryonic stem cells into neuroectodermal precursors in adherent monoculture. *Nat. Biotechnol.* **21**(2), 183-6.

Zhang, J., and Li, L. (2005). BMP signaling and stem cell regulation. *Dev. Biol.* **284**(1), 1-11.

Zhang, S.-C., Wernig, M., Duncan, I. D., Brustle, O., and Thomson, J. A. (2001). In vitro differentiation of transplantable neural precursors from human embryonic stem cells. *Nat Biotech* **19**(12), 1129-1133.

Zimmer, B., Kuegler, P. B., Baudis, B., Genewsky, A., Tanavde, V., Koh, W., Tan, B., Waldmann, T., Kadereit, S., and Leist, M. (2011). Coordinated waves of gene expression during neuronal differentiation of embryonic stem cells as basis for novel approaches to developmental neurotoxicity testing. *Cell Death Differ.* **18**(3), 383-95.

Zimmerman, G., and Soreq, H. (2006). Termination and beyond: acetylcholinesterase as a modulator of synaptic transmission. *Cell Tissue Res.* **326**(2), 655-69.

Zimmermann, M. (2013). Neuronal AChE splice variants and their non-hydrolytic functions: redefining a target of AChE inhibitors? *Br. J. Pharmacol.* **170**(5), 953-67.